Dynamic High-latitude Ionospheric Convection: Drivers and Effects

Shasha Zou

Department of Climate and Space Sciences and Engineering (CLASP)

University of Michigan

June 23, 2016

Outline

Drivers:

- Solar Wind and IMF drivers
- Modification of convection due to magnetospheric internal processes

Effects:

- Neutral dynamics effects
- Uplifting/downshifting effects
- Structuring the polar cap ionosphere
- Ion-neutral coupling within SAPS/SAID

The Geospace System

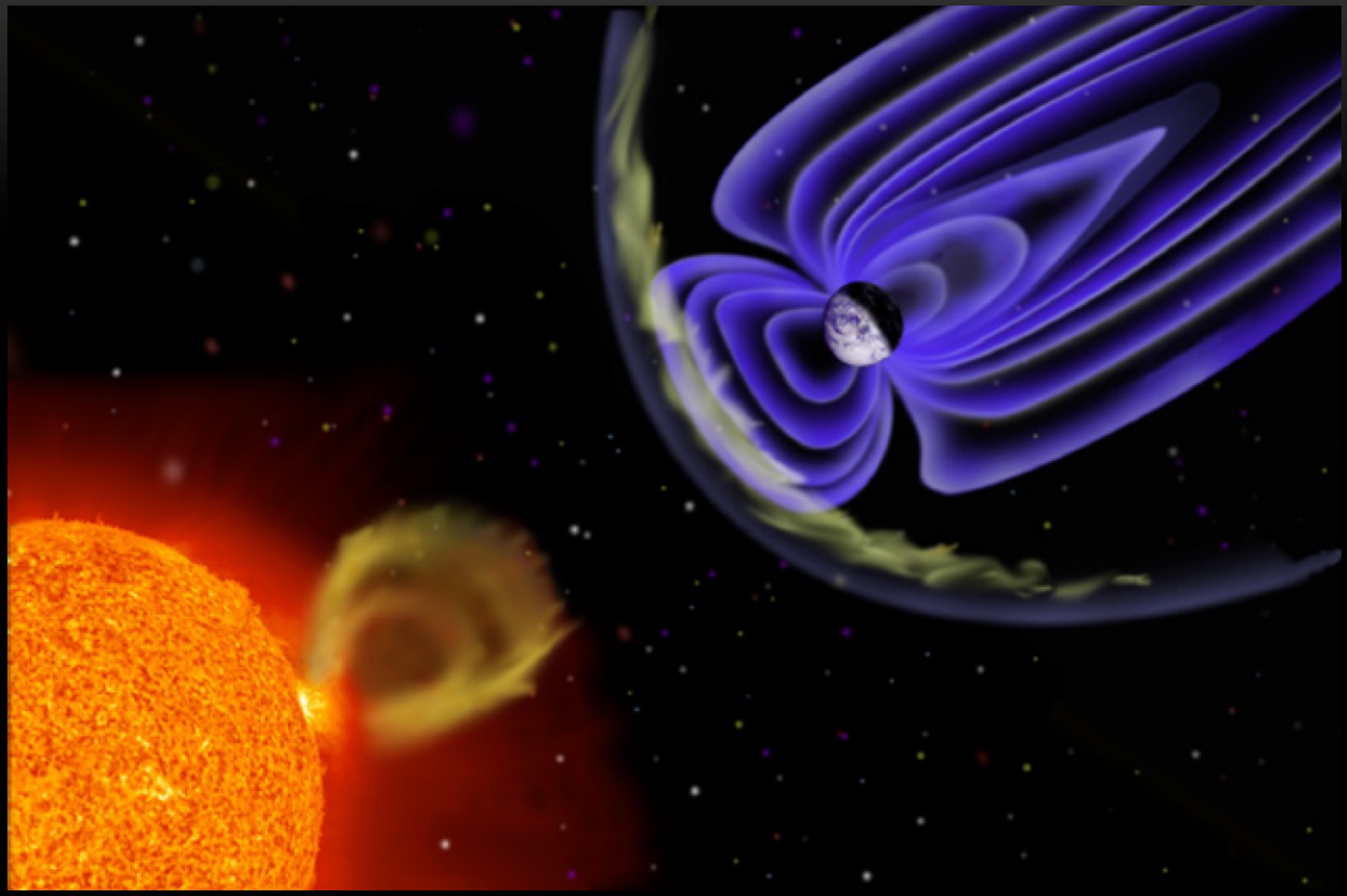

- The solar wind and IMF shape and structure the Earth magnetosphere
- Dayside magnetopause compressed
- Nightside magnetotail elongated

Magnetospheric and Ionospheric Convection: Fluid Description

Noon-Midnight Meridional Plane

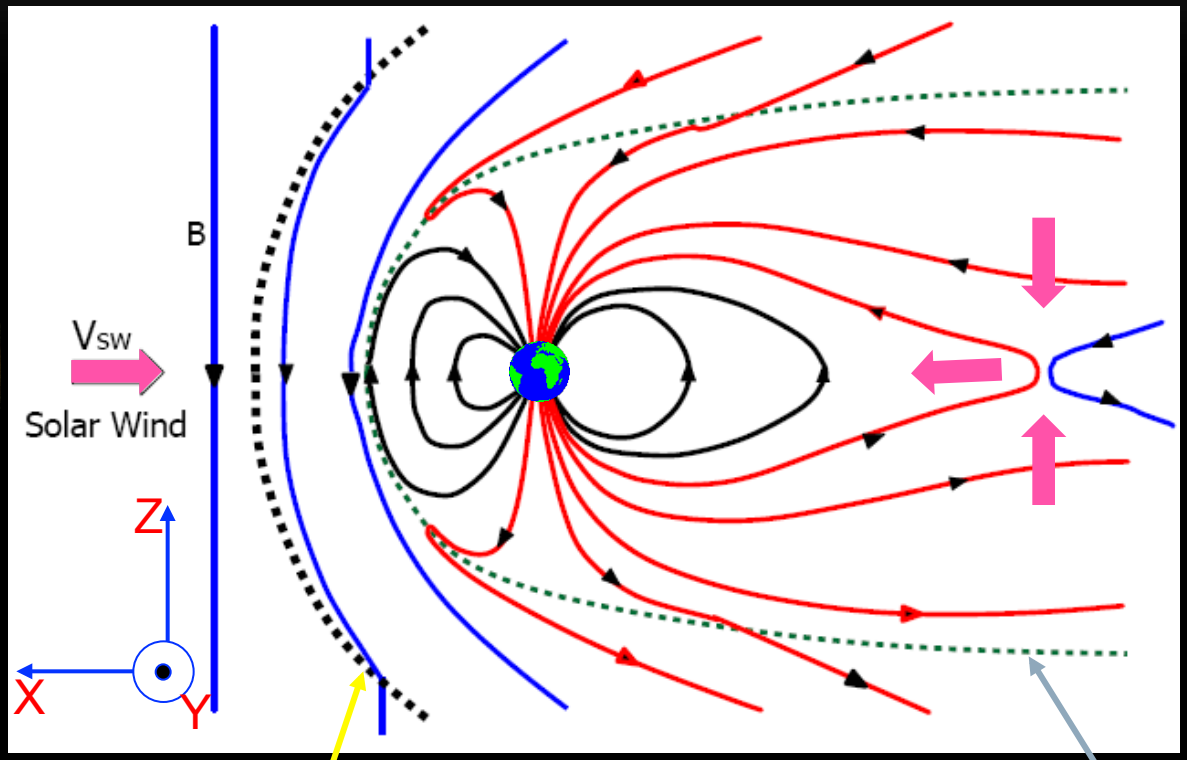

Ionosphere

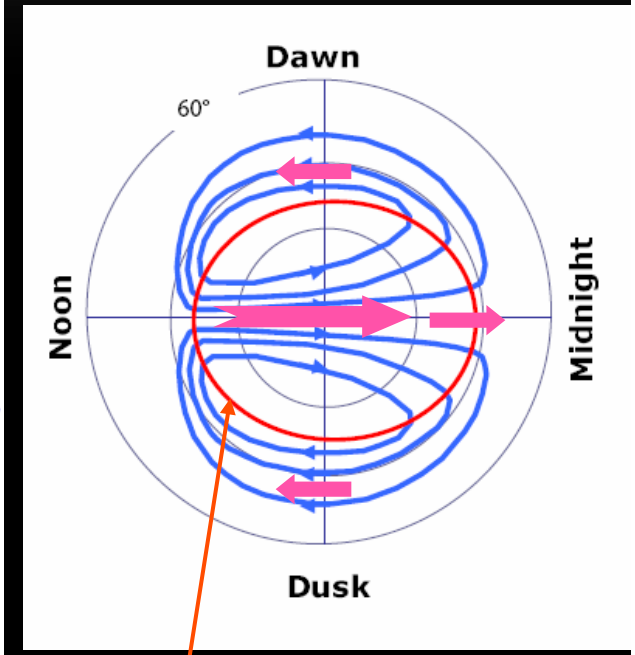

Modified from G. Lu 2005 GEM Tutorial

Bow Shock

Magnetopause

Open-Closed Field Line Boundary (OCB)

- Reconnection model proposed by J. Dungey [1961]
- Major energy and momentum coupling mechanism between the solar wind and magnetosphere

Magnetospheric and Ionospheric Convection: Fluid Description

Noon-Midnight Meridional Plane

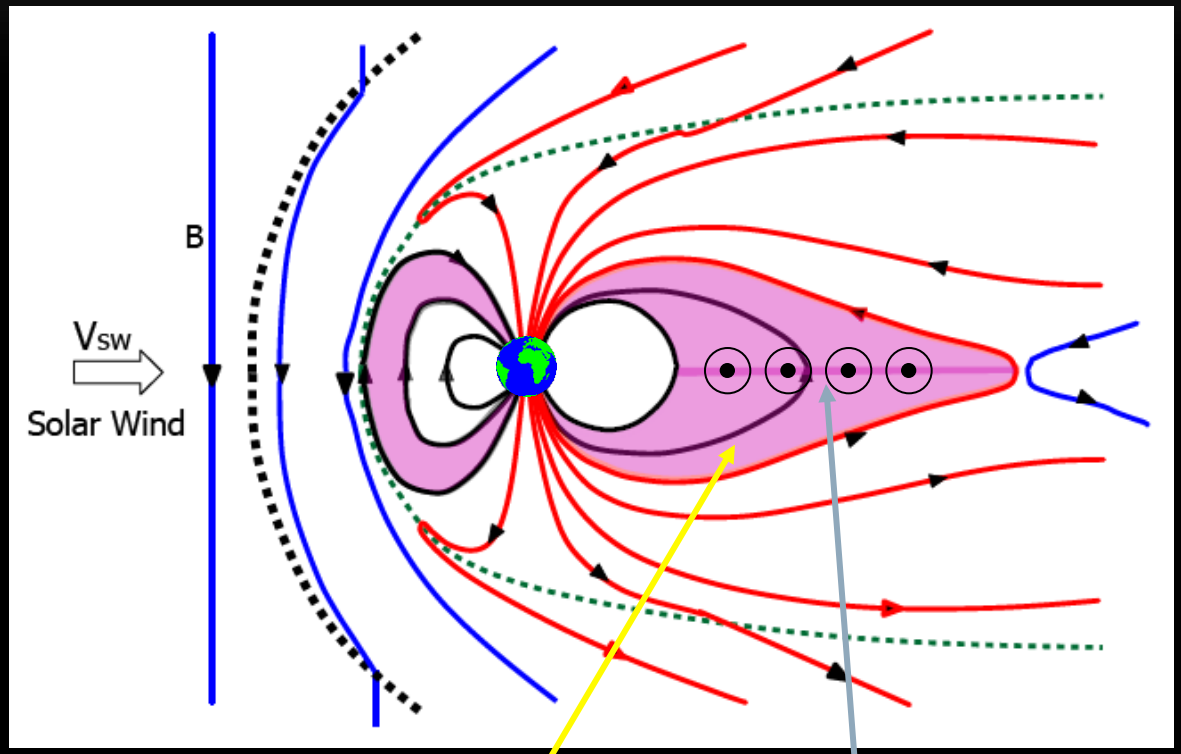

Ionosphere

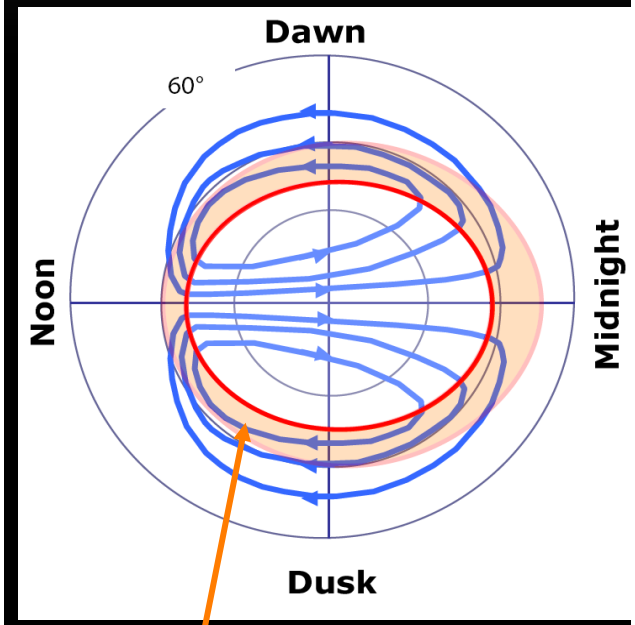

Auroral Oval

Plasma Sheet

Cross Tail Current

Viscous Interaction

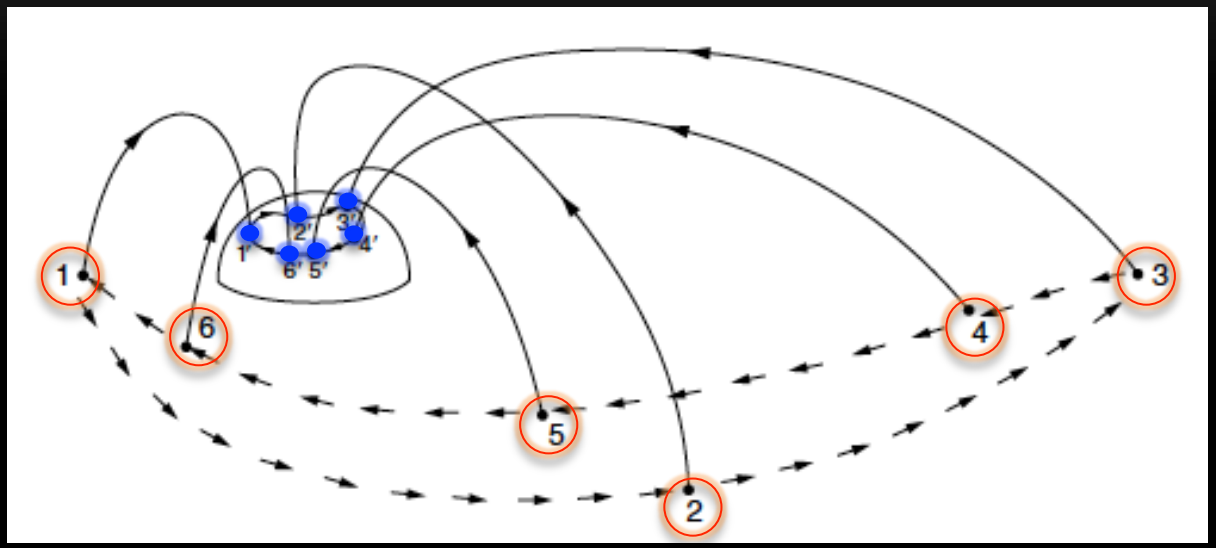

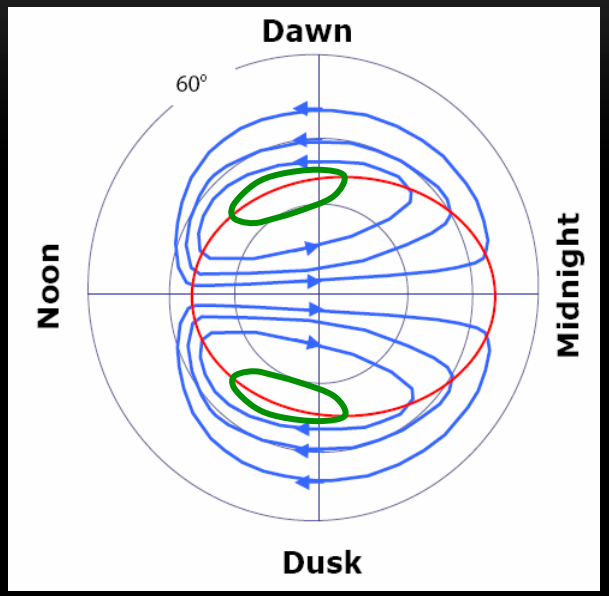

- Proposed by W. I. Axford, [1964]
- Viscous interaction moves closed field lines anti-sunward in the low-latitude boundary layer and sunward in the plasma sheet.
- Believed to play a major role under northward IMF condition and a minor role compared to dayside reconnection under southward IMF condition

High-latitude Reconnection under Northward IMF

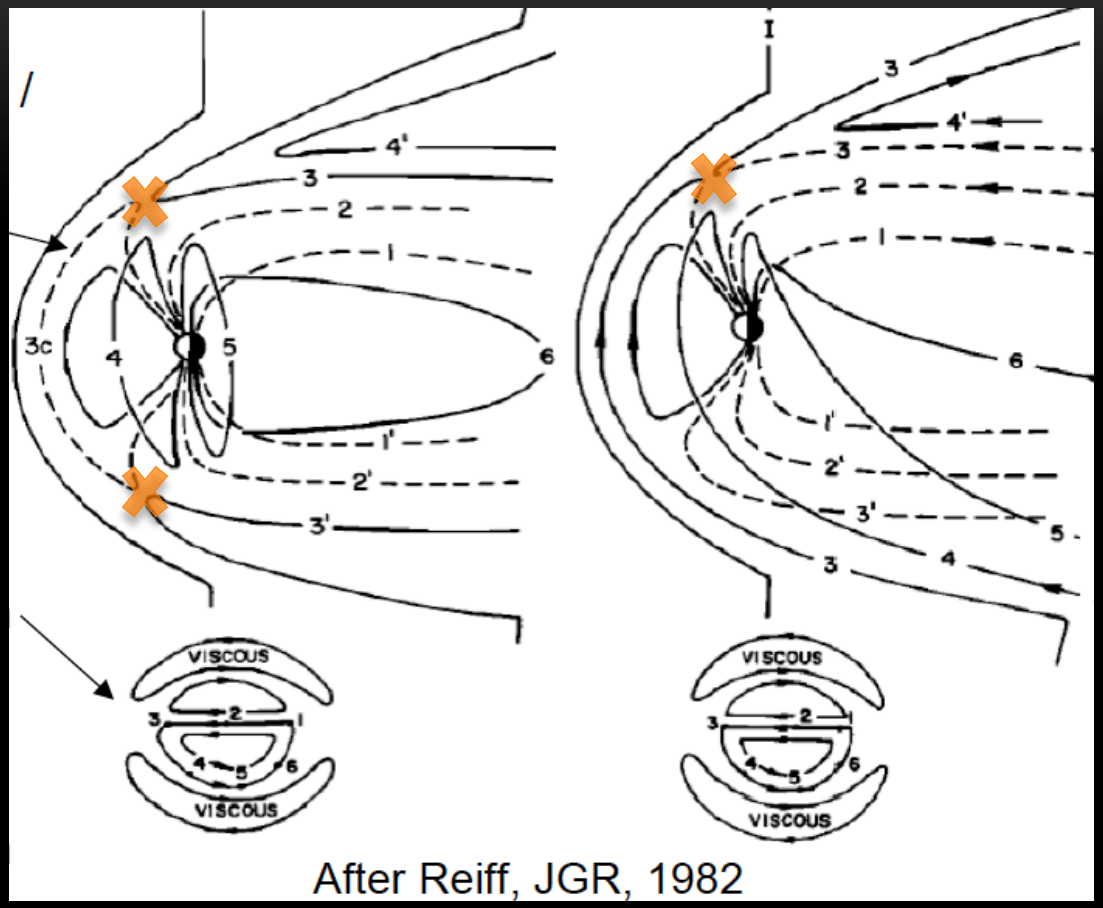

After Reiff, JGR, 1982

- Solar wind-magnetosheath plasma enters the magnetosphere through high-latitude reconnection.
- Result in complex convection pattern

Altitude Dependence of Ion and Electron Drifts in the Ionosphere

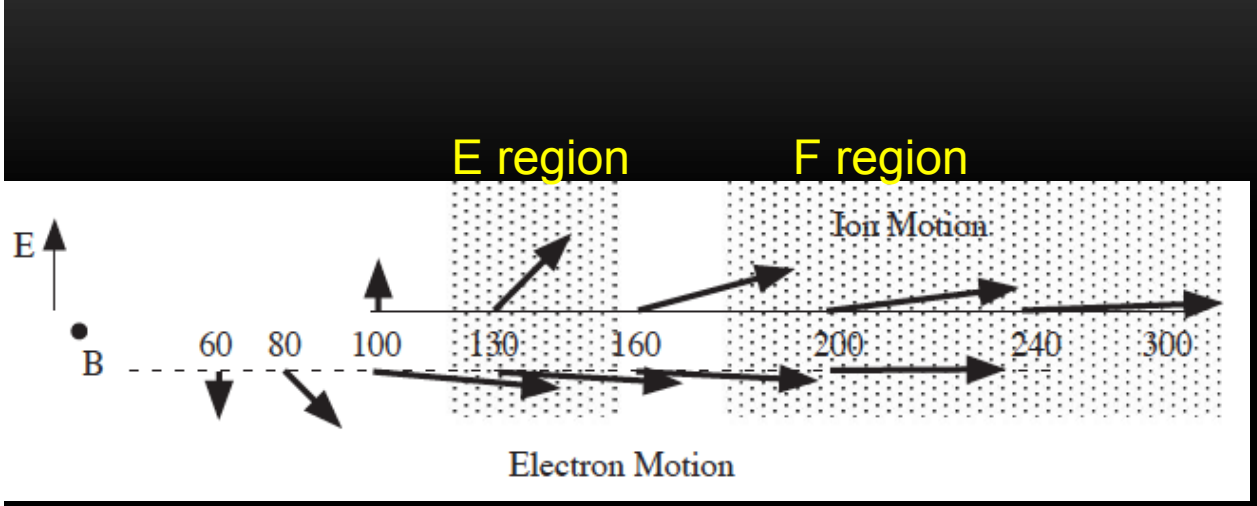

Heelis, 2004

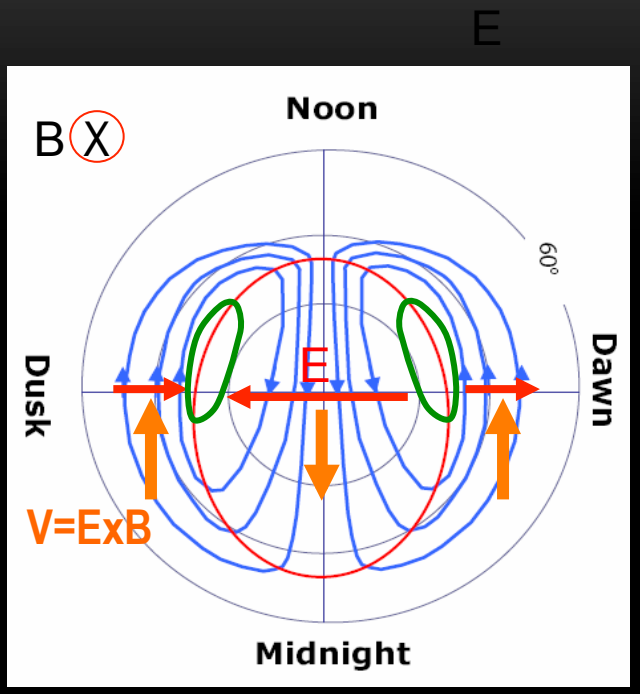

- In the F region, plasma drifts in the ExB direction, and no horizontal currents flow.
- In the lower E region, electrons drift in the ExB direction. Ions drift roughly in the direction of the electric field.
- As altitude increases from lower E region, the ion drift velocity rotates toward the ExB direction because the ion–neutral collision frequencies decrease with altitude.
- Horizontal currents flow in the E region.

IMF Dependence of Convection Pattern

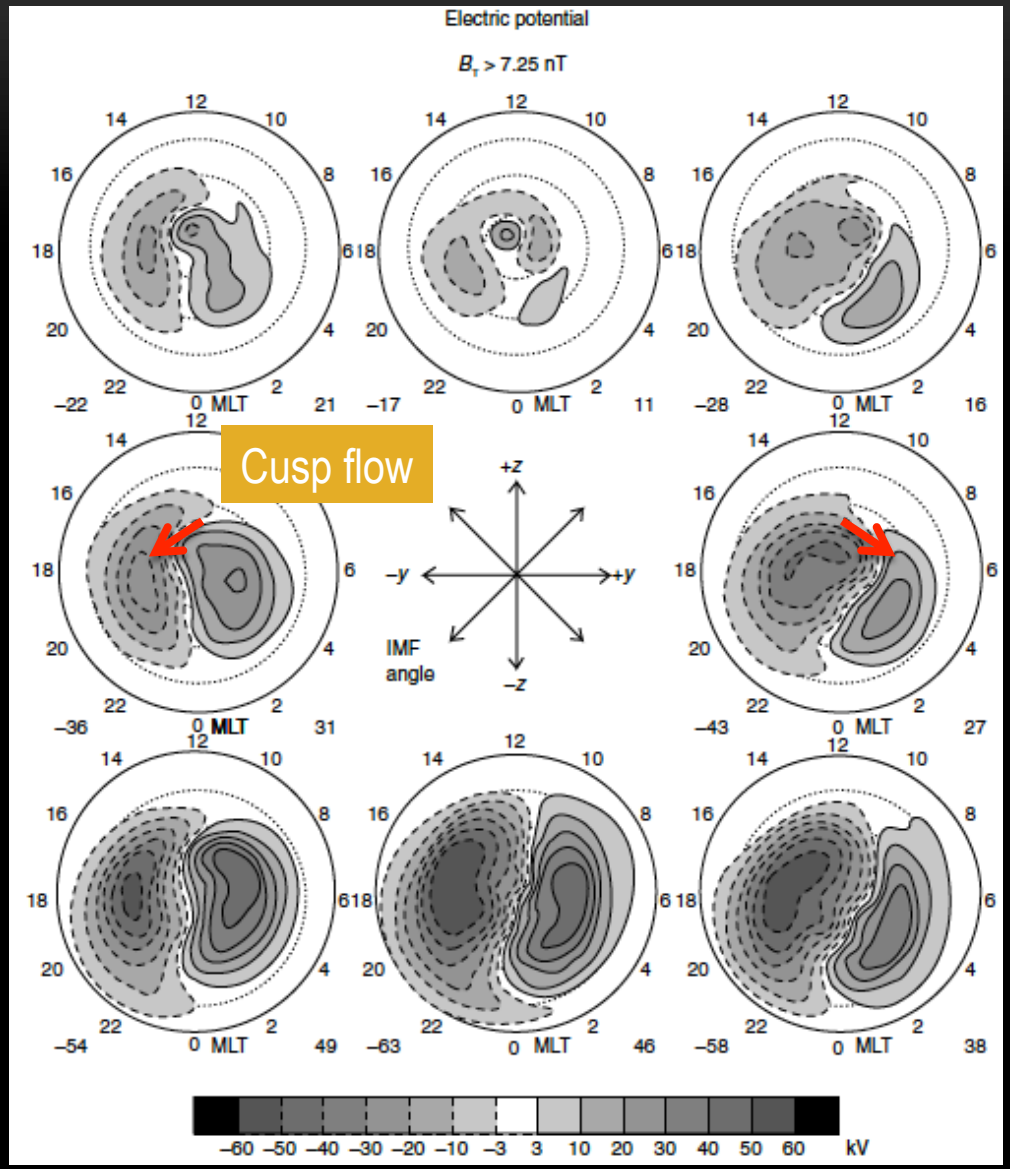

Weimer, 1995

- Without corotation
- 2-cell convection pattern during southward IMF
- 3 or 4-cell convection pattern during northward IMF
- Cusp flow direction depends on the sign of IMF By

Electric Field in the Equatorial Plane in Inertial Frame

$$\Phi = -E_o y - \frac{B_o \omega_E R_E^3}{r}$$

Uniform convection E field

Corotation E field

- The total electric field is the sum of uniform convection electric field and the corotation electric field.
- The separatrix is the boundary between closed and open drift trajectories.

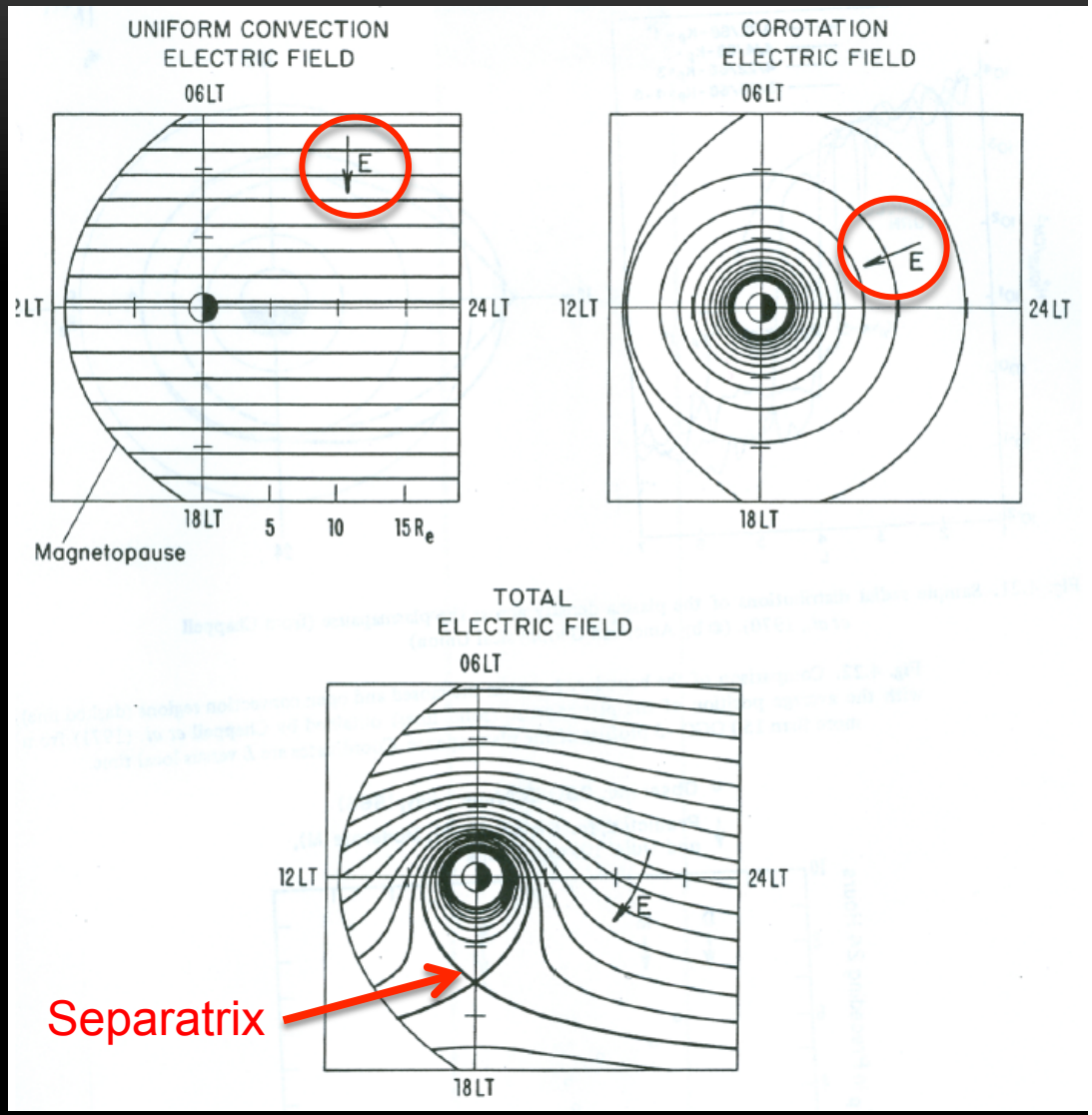

Lyons and Williams, 1984

Energetic Particle Drifts

$$\phi_{\text{eff}}^{\text{hot}} = -E_0 r \sin\varphi + \frac{\mu B_0 R_E^3}{q r^3}$$

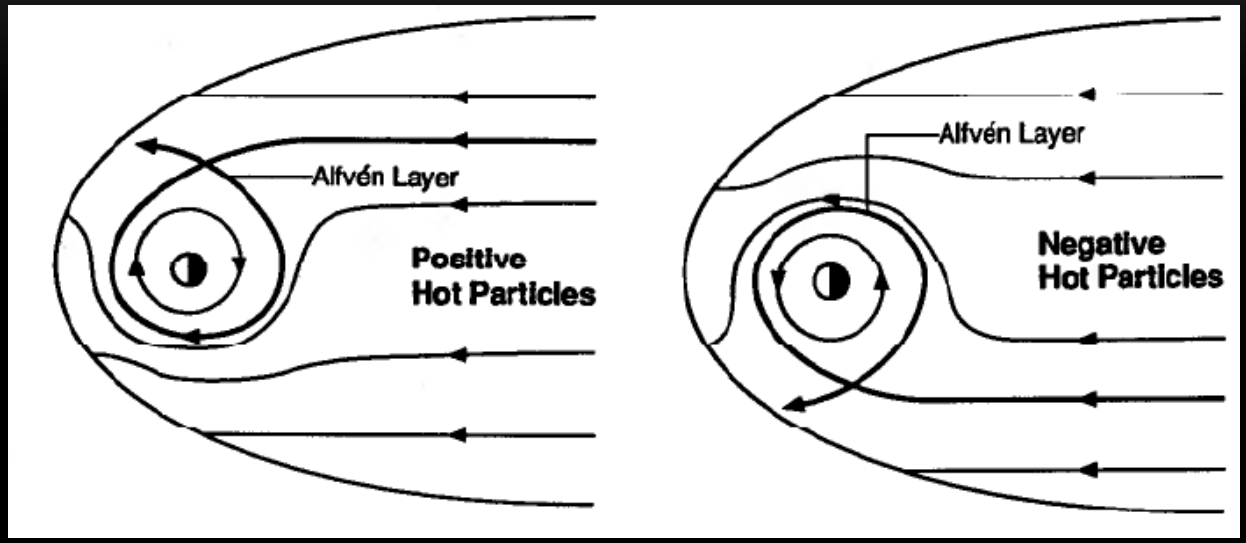

Kivelson and Russell, 1995

- Energetic particles are subject to gradient and curvature drift.
- Positively charged particles gradient and curvature drift towards the dusk side.
- Negatively charged particles gradient and curvature drift towards the dawn side.

Shielding in the Inner Magnetosphere

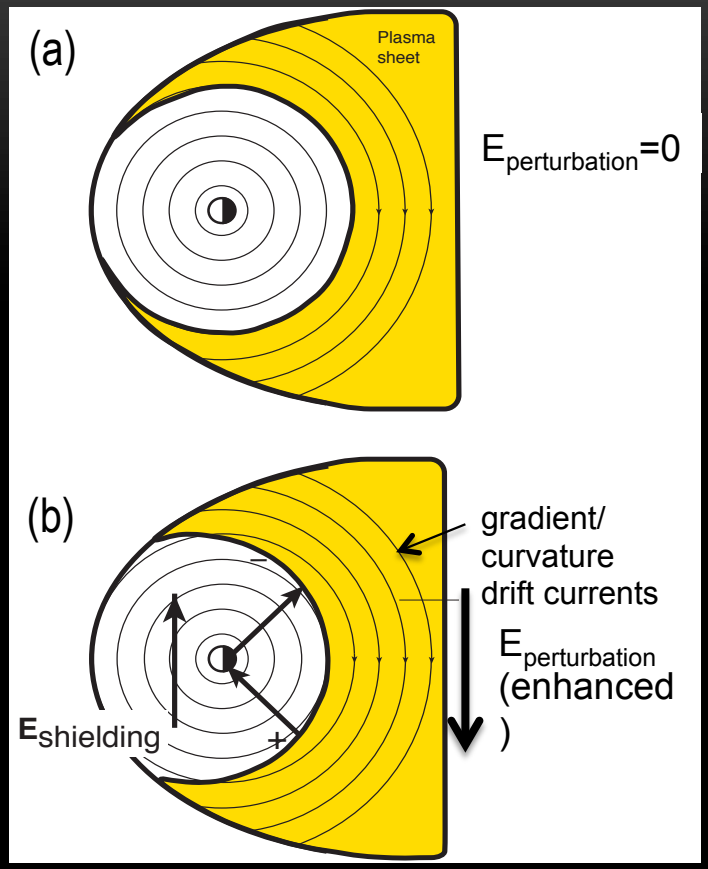

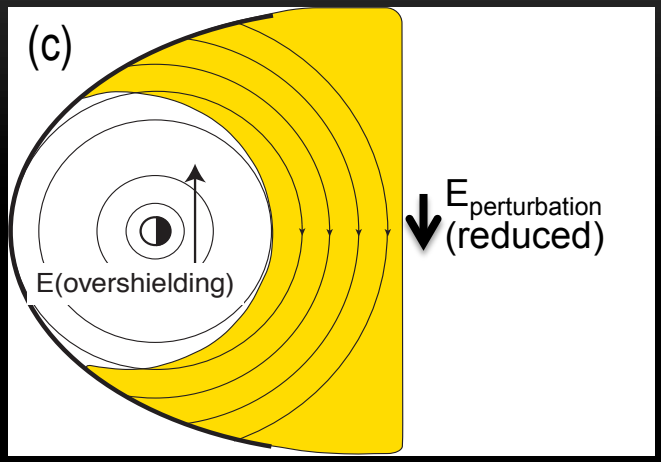

Wolf et al., 2007

a) An equilibrium configuration with no convection electric field
b) Convection E field increases and moves the inner edge of the plasma-sheet sunward. Ions drift to the duskside and electrons drift to the dawnside. The shielding E field, in effect, reduces the imposed convection E field in the inner magnetosphere.
c) Shielding electric field is stronger than the convection E field.

Harang Reversal and SAPS

Equatorial Plane

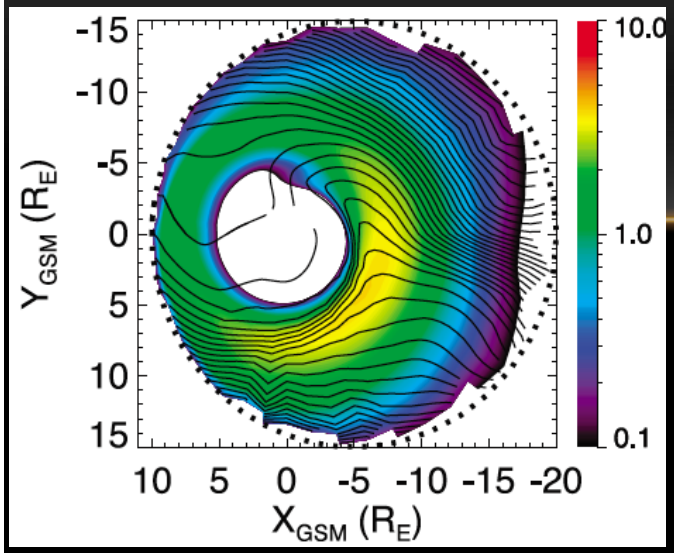

Ionosphere

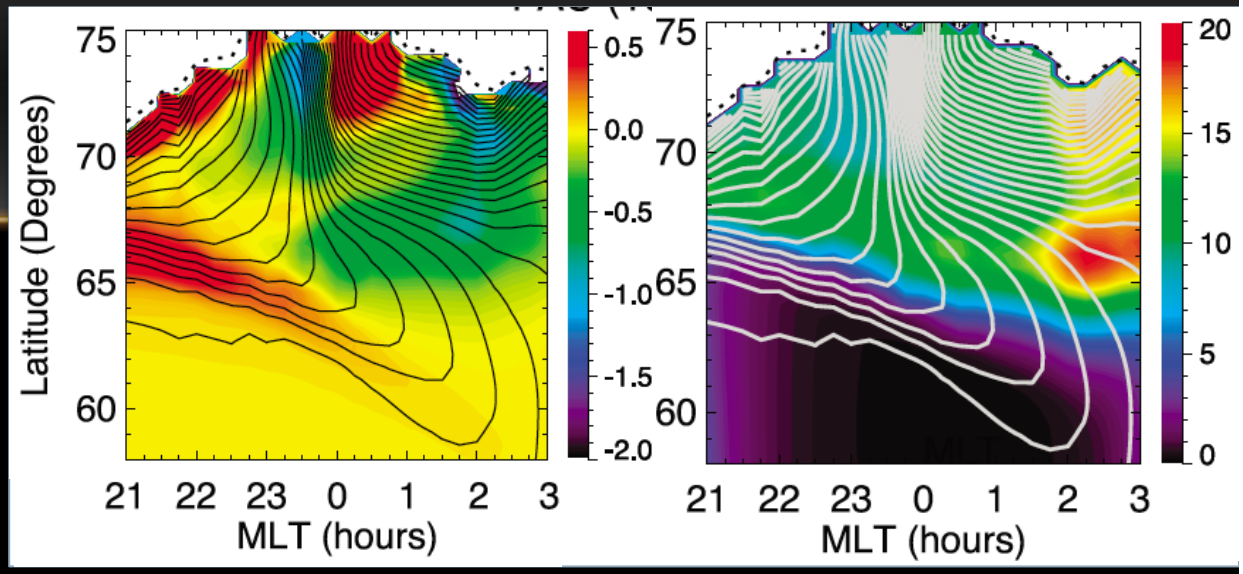

Gkioulidou et al. 2011

Aspects of the shielding process:

- Partial westward ring current forms across the night side.
- Field-aligned Region-2 currents, flow up/down from dawnside/duskside ionosphere near the plasma sheet inner edge.
- Convection features, including the Harang reversal and SAPS, form during this process.
  - Overlap between the upward and downward Region-2 FACs necessary for the Harang reversal formation [*Gkioulidou et al.* 2009, 2011].

Effects Part 1: Neutral Dynamics Effects

Ion-neutral coupling

- Convecting ionosphere can be a significant source of momentum and energy for the thermosphere via ion–neutral collisions.
- Resulting interactions act to modify the thermospheric circulation, temperature, and composition, which, in turn, affects the ionosphere.
- Extent of the coupling depends on plasma density. For plasma densities of 10^3 to 10^6 cm^{-3}, the characteristic time constant for accelerating the thermospheric particles ranges from 200 hours (several days) to 10 minutes.

Temporal change of ion temperature:

$$\frac{\partial}{\partial t} T_i = \nu_{in}\left(-T_i + T_n + \frac{M_n}{3k} (\bar{v} - \bar{u})^2 \right)$$

Time scale for ions to respond to frictional heating:

$$\tau \propto \frac{1}{\gamma_{in}}$$

A few seconds to a few tens of seconds

Time scale for neutrals to respond to frictional heating:

$$\tau \propto \frac{1}{\gamma_{ni}} = \frac{n_n m_n}{n_i m_i \gamma_{in}} \gg \frac{1}{\gamma_{in}}$$

Because the neutral density is much higher than the ion density, the time scale for neutrals is much longer than that of ions.

Evidence of Ion-Neutral Coupling at High Latitudes

Southward IMF

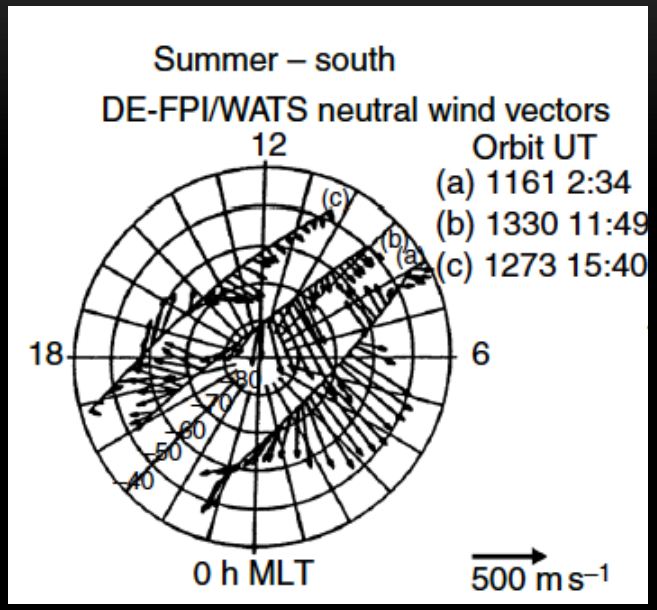

Schunk and Nagy, 2009

Northward IMF

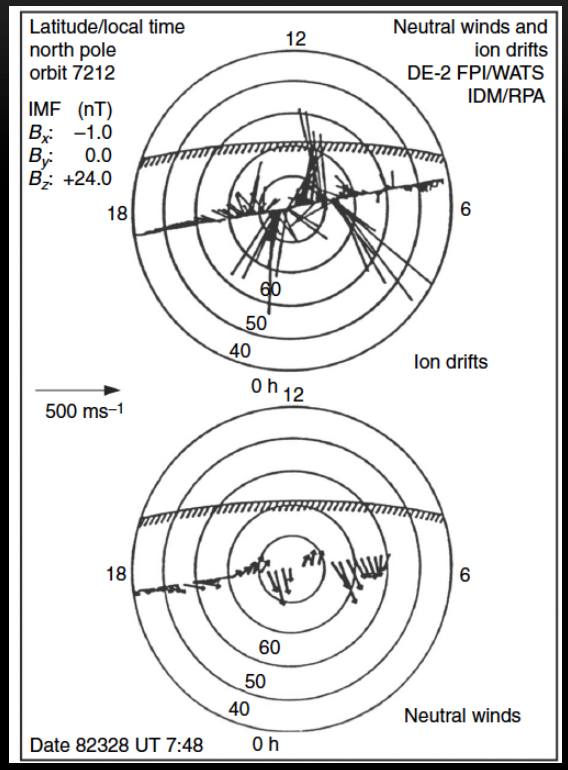

- High-latitude thermospheric wind pattern mimics the plasma convection pattern.
- The wind speed is typically smaller than plasma convection speed but much greater than expected if solar heating was the only process driving the flow.

Neutral Flywheel Effects

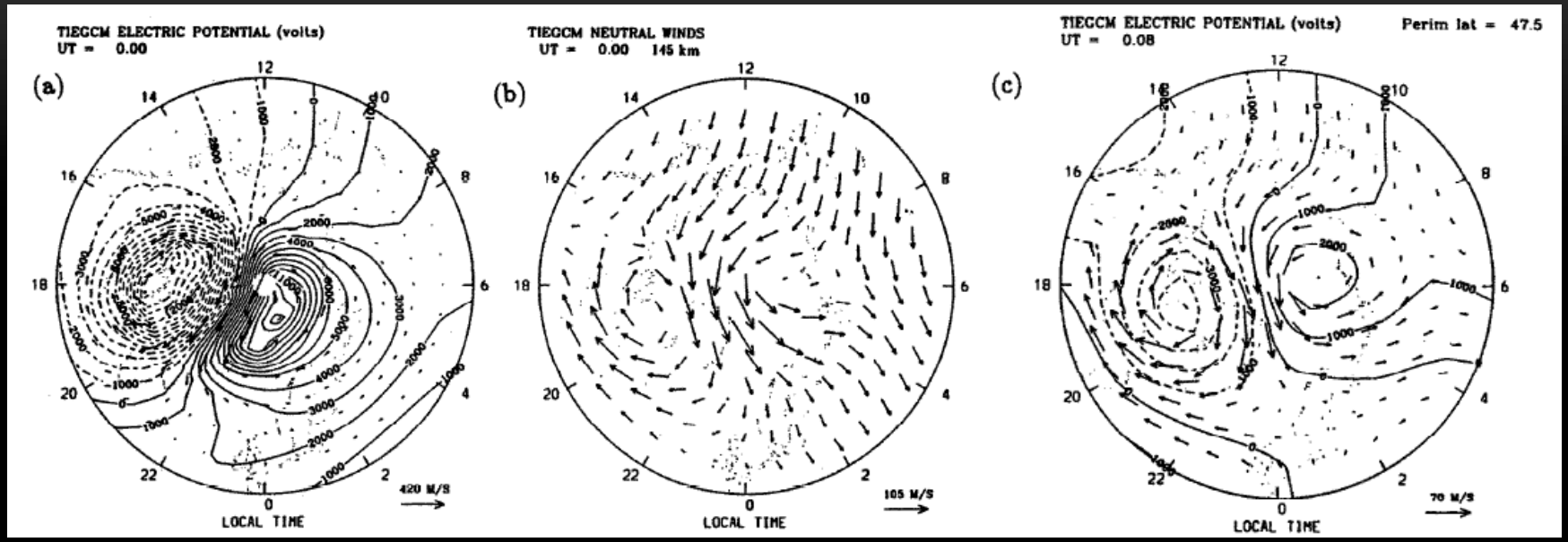

Richmond and Roble, 1997

- High-latitude winds on average play a secondary role in the magnetosphere-ionosphere electrodynamic coupling.
- However, they can play a more important role immediately following a period of high magnetic activity.
- Neutral winds tend to maintain the ion convection pattern after the external sources are cut-off.

Effects Part 2: Uplifting/downshifting Effects

Decompose ExB Drift to Horizontal and Vertical Drifts

with corotation

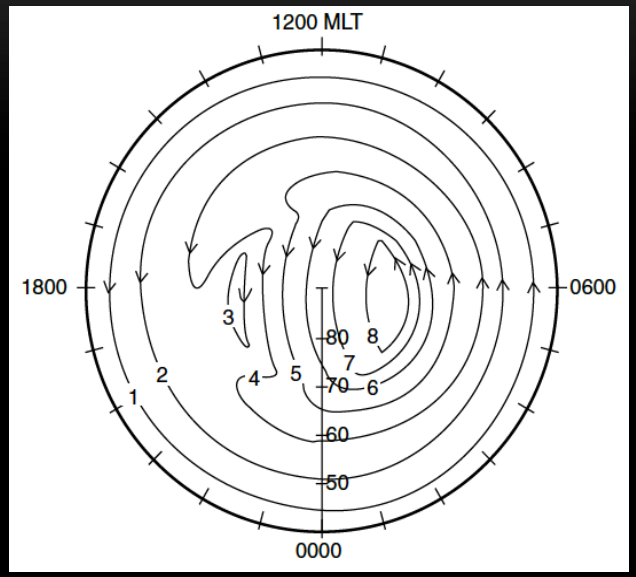

horizontal drift (m/s)

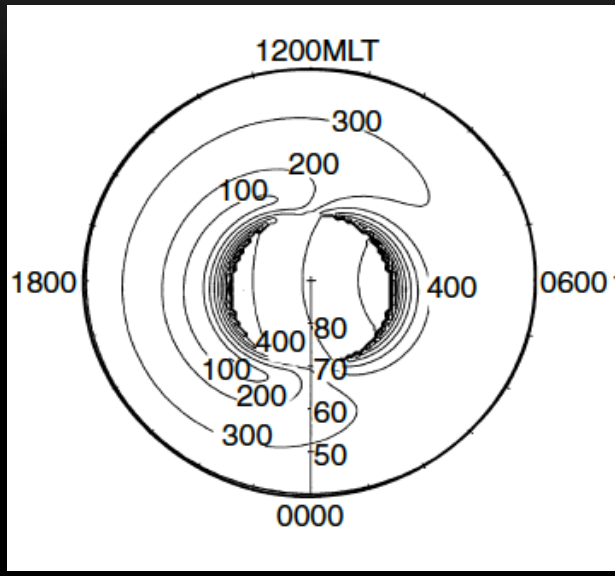

vertical drift (m/s)

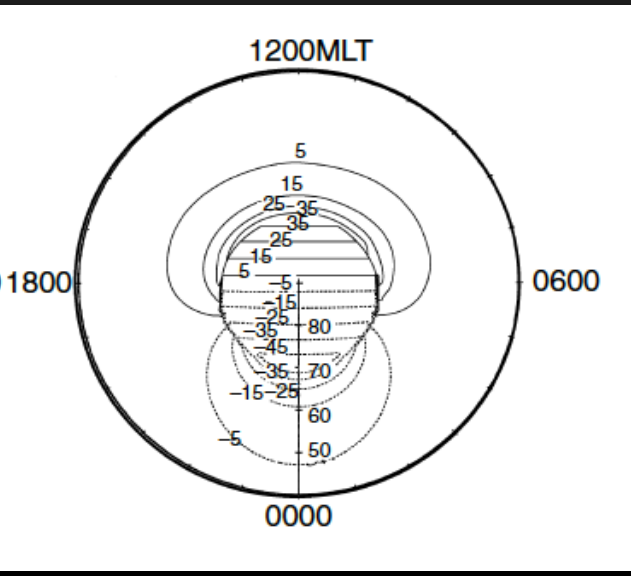

Schunk and Nagy, 2009

- ExB drift has both horizontal and vertical components when the magnetic field line is not purely vertical.
- During southward IMF, the vertical drift is upward on the day side and downward on the night side.

Induced Vertical Plasma Drift

(a)Vertical force

(b) Equatorward meridional neutral wind

(c) Eastward electric field

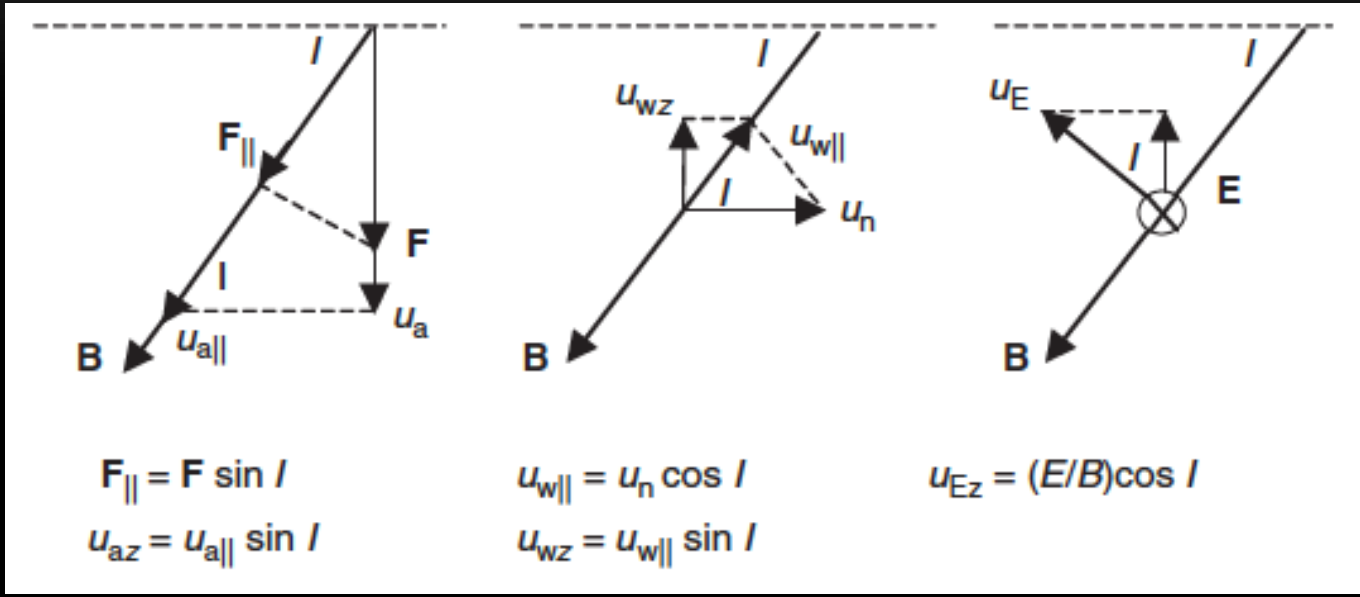

$F_{\parallel} = F \sin I$

$u_{az} = u_{a\parallel} \sin I$

$u_{w\parallel} = u_n \cos I$

$u_{wz} = u_{w\parallel} \sin I$

$u_{Ez} = (E/B)\cos I$

Total vertical plasma drift speed:

$$u_{iz} = \frac{E}{B}\cos I + u_n \sin I \cos I - \sin^2 I D_a \left(\frac{1}{n_i}\frac{\partial n_i}{\partial z} + \frac{1}{T_p}\frac{\partial T_p}{\partial z} + \frac{1}{H_p} \right)$$

(c) (b) (a)

Schunk and Nagy, 2009

- Vertical plasma drift is determined by the interplay between convection electric field, thermospheric wind, and ambipolar diffusion.

Major Chemical Reactions in the F-region

$$O^+ + N_2 \xrightarrow{K1} NO^+ + N \quad (1)$$

$$O^+ + O_2 \xrightarrow{K2} O_2^+ + O \quad (2)$$

$$O^+ + NO \xrightarrow{K3} NO^+ + O \quad (3)$$

$$NO^+ + e^- \xrightarrow{K4} O + N \quad (4)$$

$$O_2^+ + e^- \xrightarrow{K5} O + O \quad (5)$$

$$O^+ + e^- \xrightarrow{K6} O \quad (6)$$

- O^+ is the dominant ion in the F region.
- Major chemical reactions in the F-region are charge exchanges (1-3) and dissociative recombinations (4-5).
- Radiative recombination (6) is very slow compared to other reactions.
- Moving F-layer plasma up or down by the induced vertical plasma drift can affect the life time of plasma by moving away or towards regions of denser neutrals.

Density Variability within Storm-Enhanced Density (SED)

N_e altitude profile from PFISR

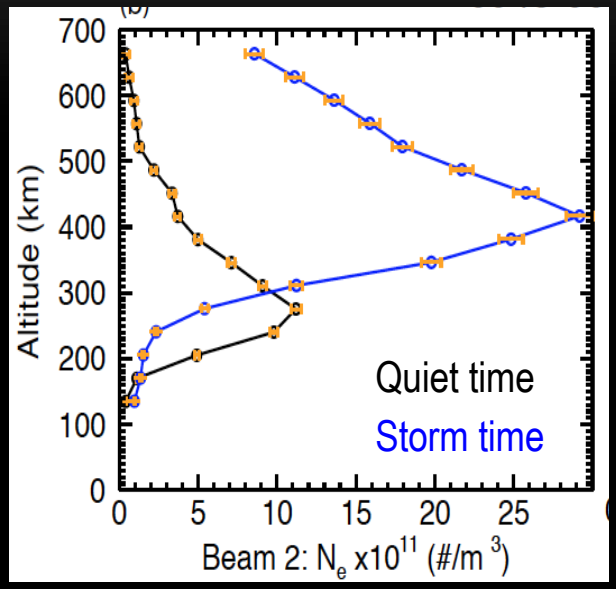

Zou et al. 2013

2D GPS VTEC maps during storm

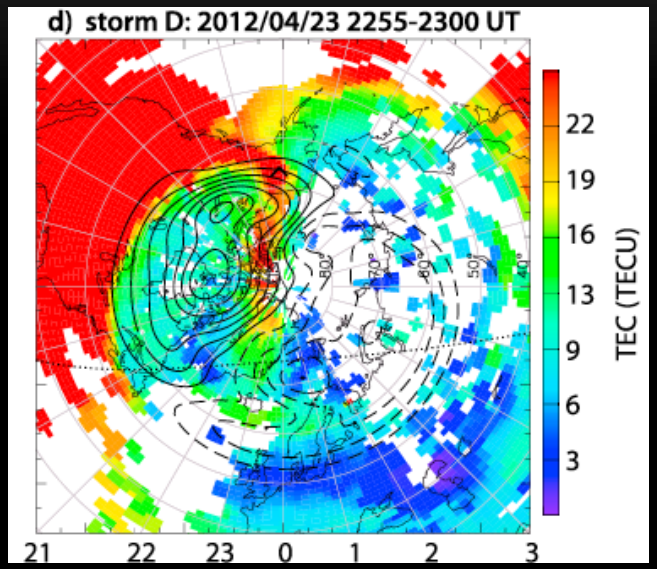

Zou et al. 2014

- Result of magnetosphere-ionosphere-thermosphere coupling processes;
- Important mechanism for transporting solar produced high density plasma into low density polar cap and nightside auroral region;

Vertical Plasma Drift within SED

2011 Oct. 24-25 storm IMF southward turning

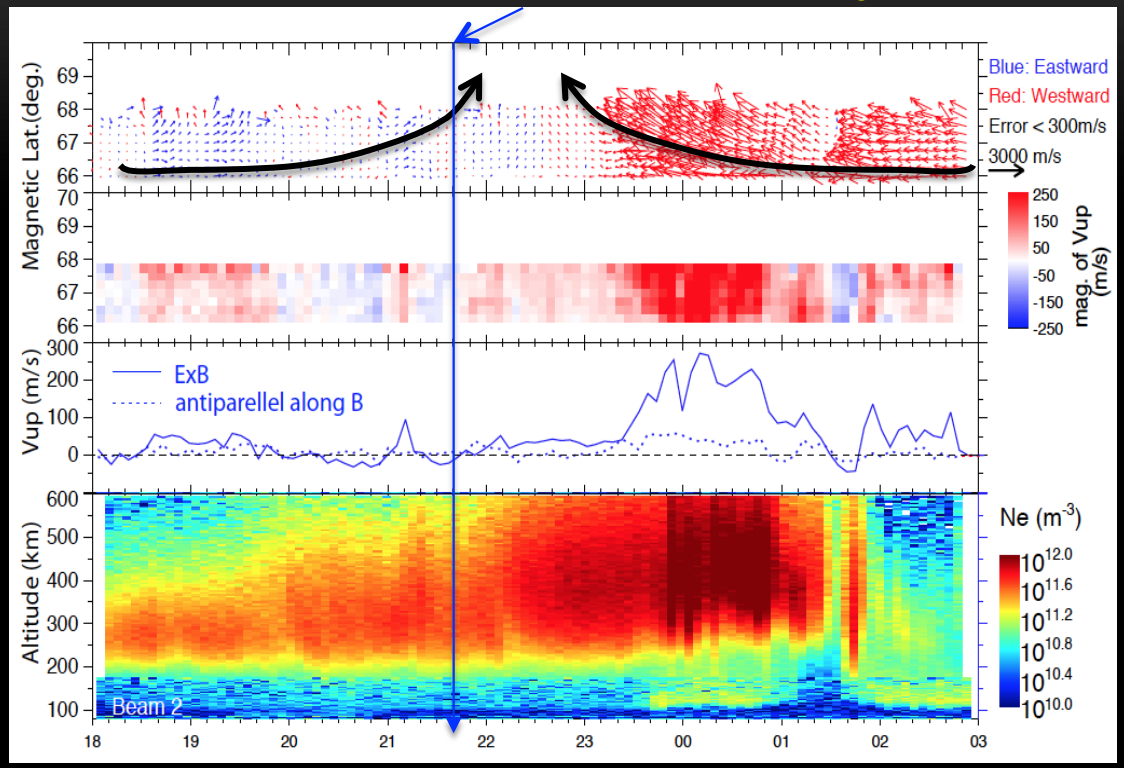

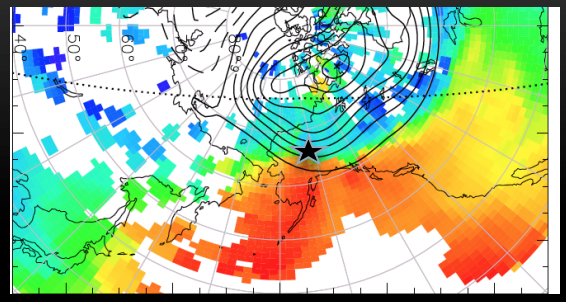

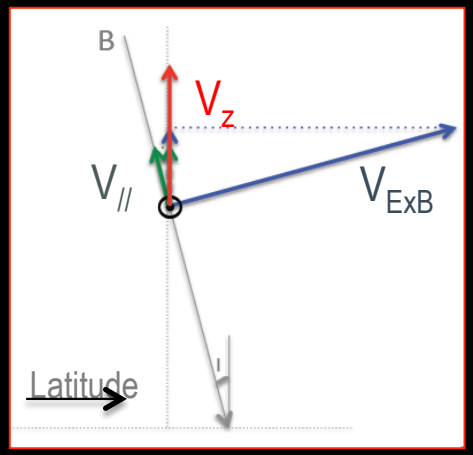

Zou et al. 2013

- Both convection flow and field-aligned drift contribute to the upward vertical drift.
- In this case, convection flow plays a major role.

Vertical Plasma Drift within SED Plume

2012 Nov. 13-14 storm

Further IMF southward turning

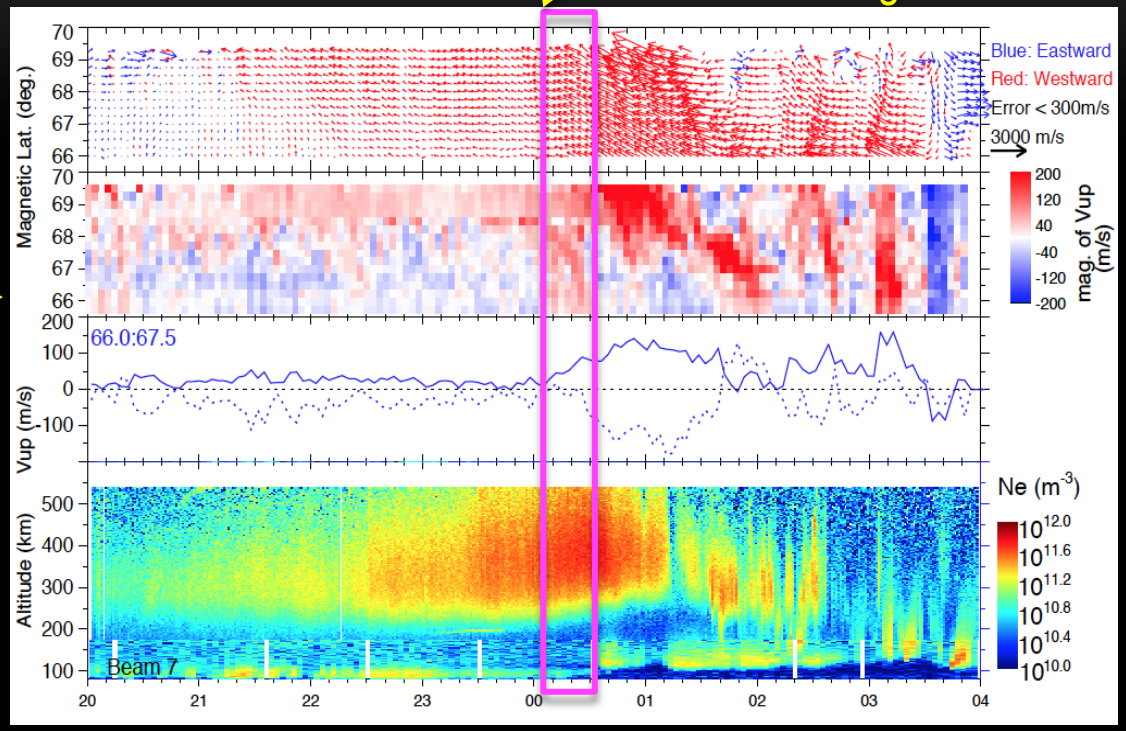

Zou et al. 2014

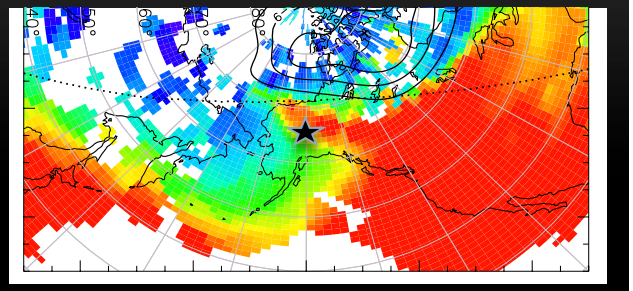

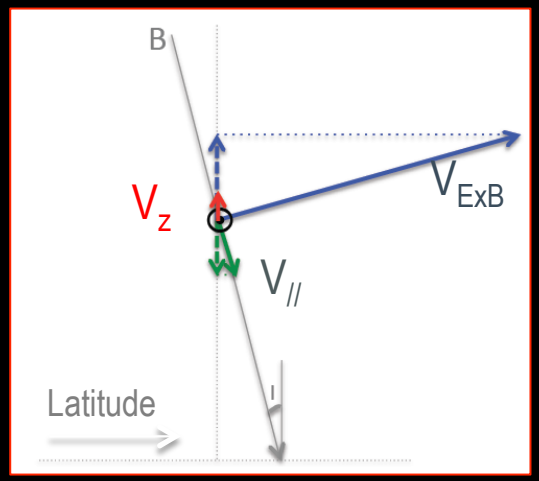

- Upward vertical flows are due to penetration electric field after sudden southward turning of the IMF.

Vertical Plasma Drift within SED Plume

2012 Nov. 13-14 storm

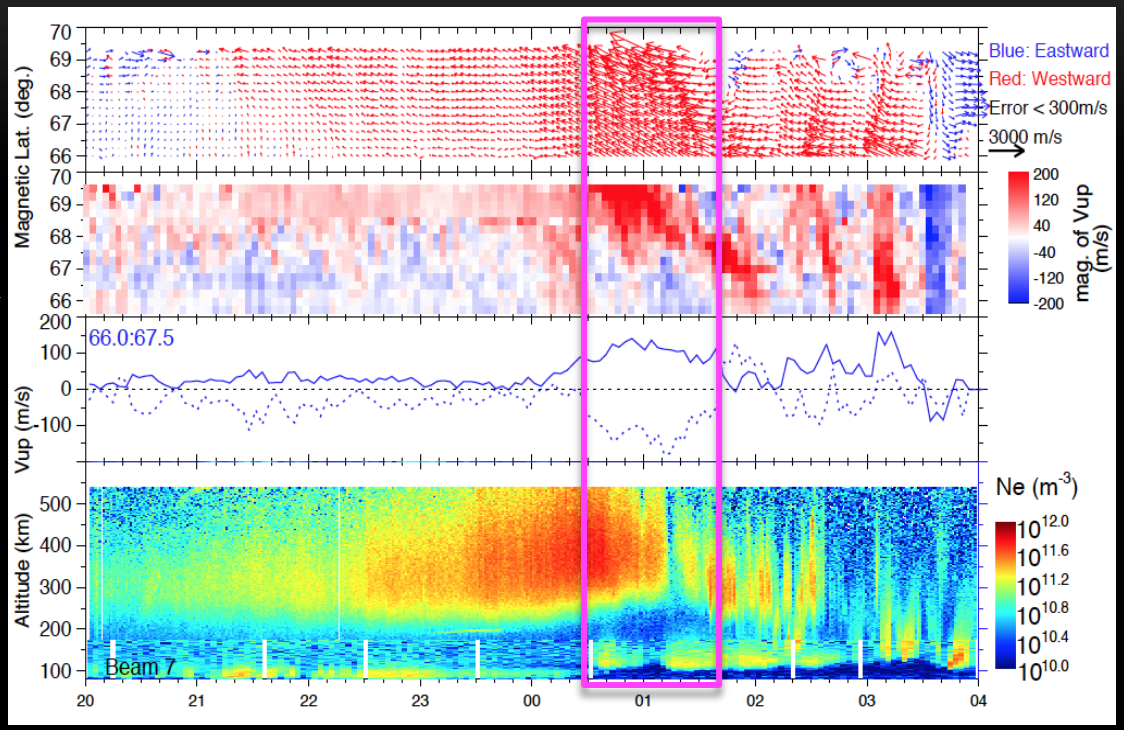

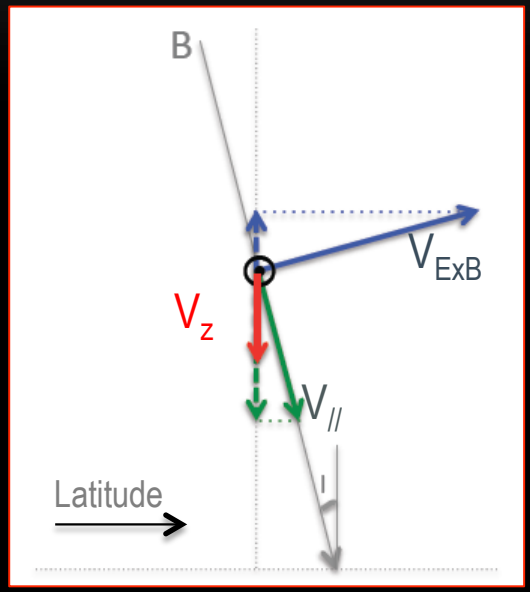

Zou et al. 2014

- Field-aligned downward flows largely increased, overturned the lifting due to convection flow and resulted in net downward vertical flows.
- These net downward vertical flows push plasma to lower altitudes, where higher recombination rates lead to plasma density decrease.
- Both poleward thermospheric wind and enhanced downward diffusion contribute to the field-aligned downward flows.

Not Every Plume Can Make To The Polar Cap!

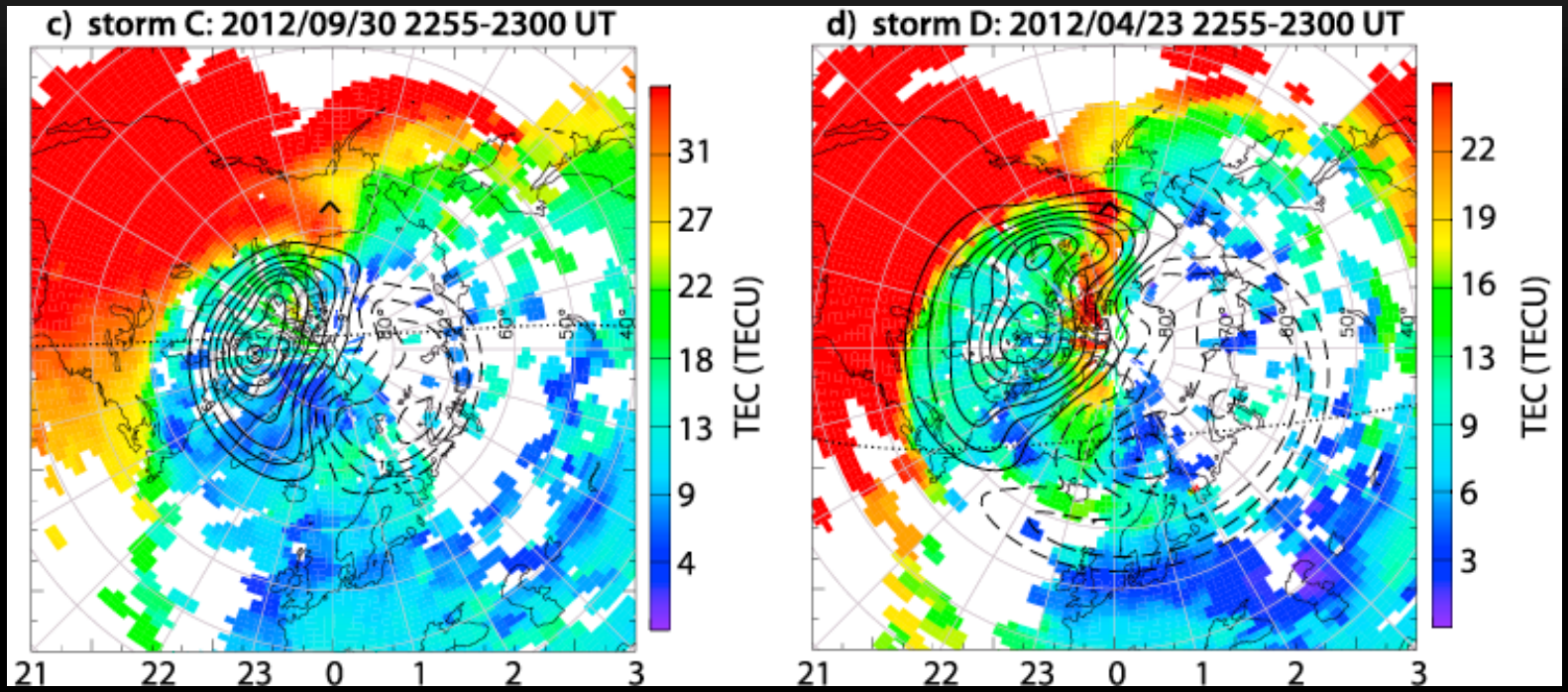

Zou et al. 2014

GITM Simulation of SED

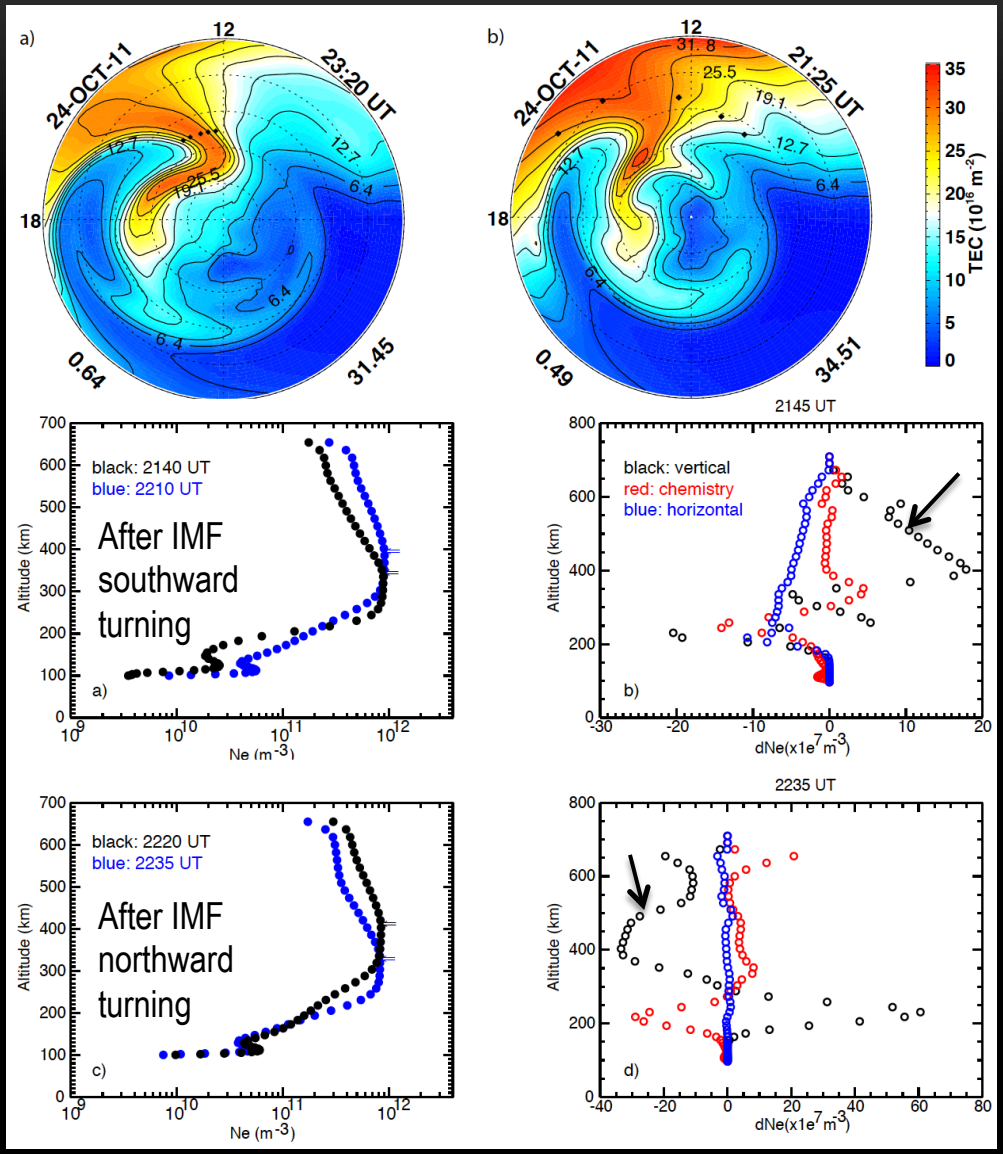

- Plasma in the same simulation column are traced backwards in time to study the origin and major loss and source mechanisms.
- F-region plasma density sensitively responds to the strength of the convection electric field.

Zou and Ridley, 2015

TDIM Simulation of SED

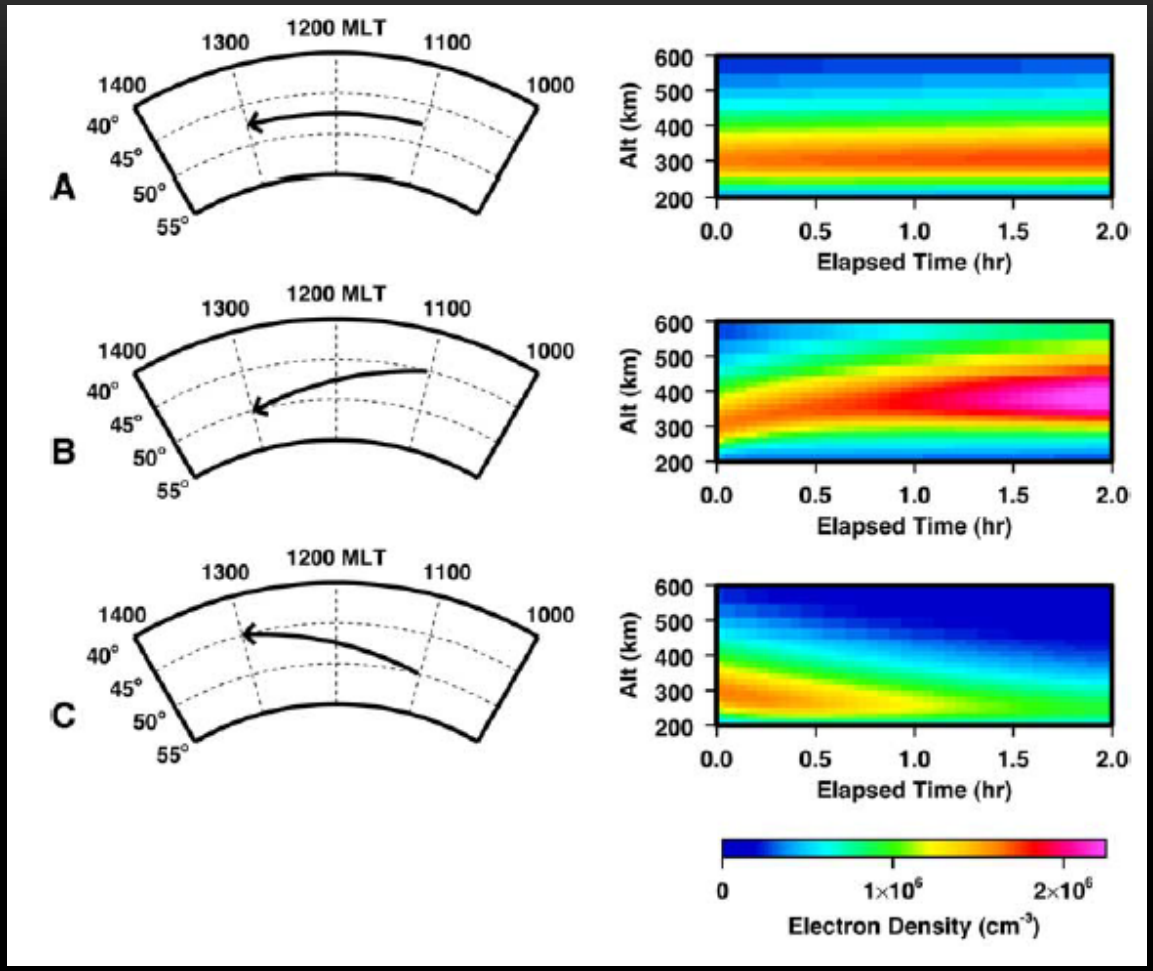

40→43 TECU change

40→70 TECU change

40→18 TECU change

Heelis et al. 2009

- Because of non-vertical magnetic field, poleward/equaterward convection leads to ionospheric density increase/decrease.

TIMEGCM Simulation of SED

Vertical drift due to electric field

Vertical drift due to meridional wind

Total vertical drift

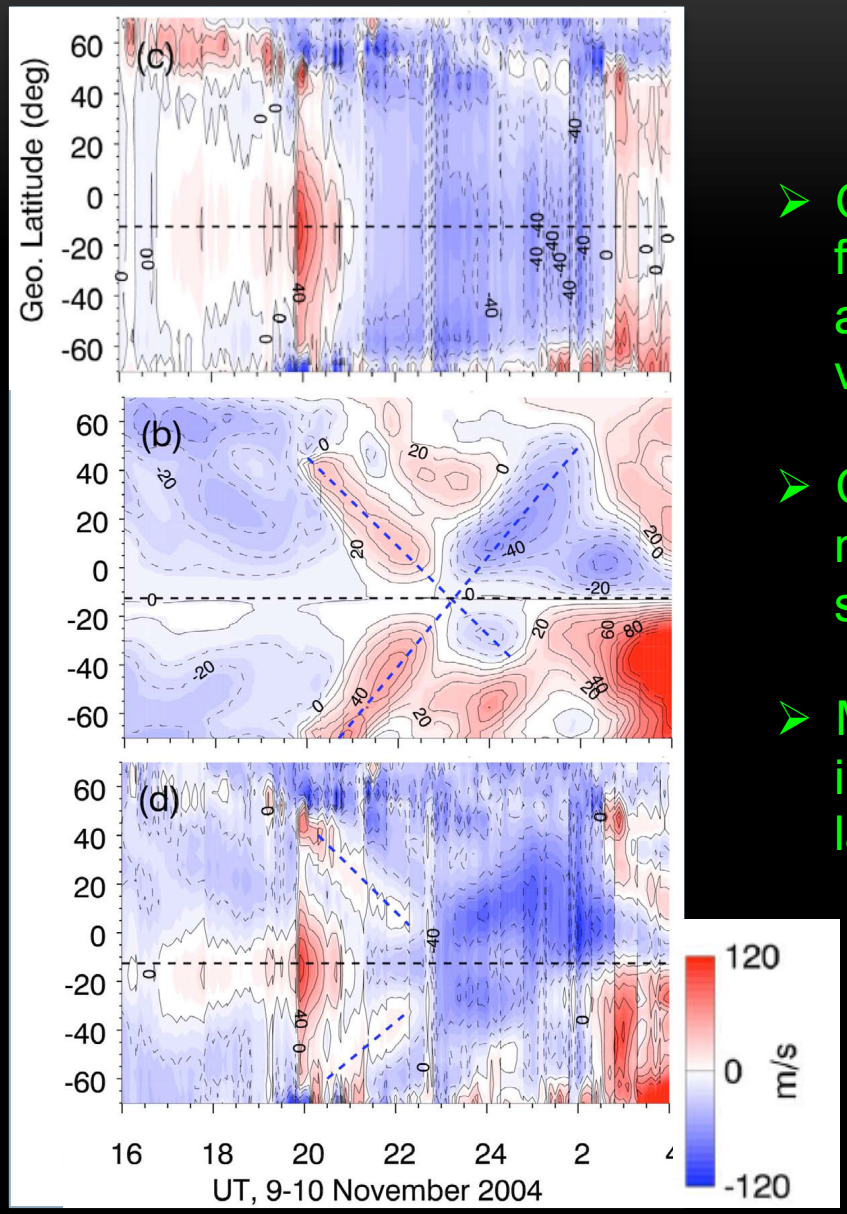

- Quantified the contributions from convection electric field and meridional wind to vertical plasma drift.
- Convection electric field is more important in the subauroral region.
- Meridional wind plays an important role at mid latitudes.

Lu et al. 2012

Coupled SAMI3-RCM Simulation of SED

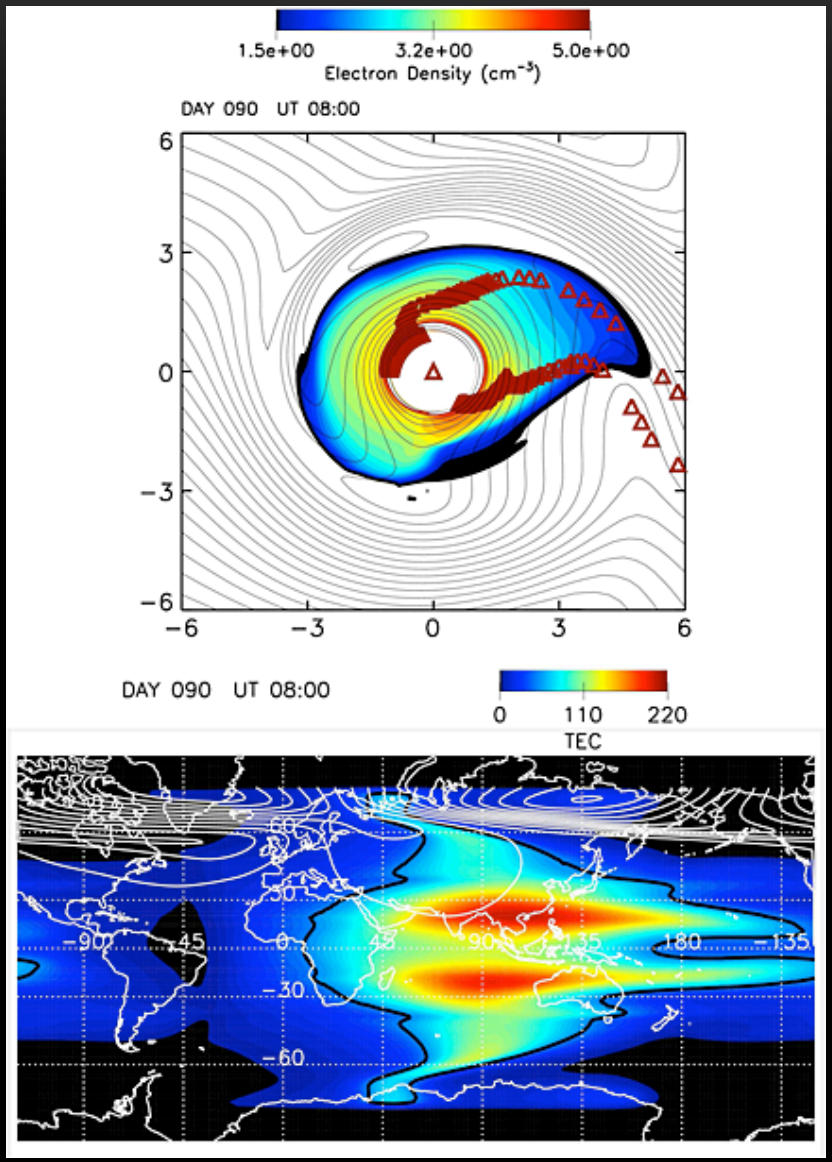

Huba and Sazykin, 2014

- Minimum D_{st} during March 31, 2001 storm reached -387 nT.
- Plasma from the expanded Appleton anomaly contributes to the formation of SED plume.

Summary Part 1

- Given non-vertical magnetic field, poleward convection flows can lift the plasma to higher altitudes where the recombination rate is lower.
- Given continuous production on the dayside, the ionospheric plasma density can increase significantly.
- Convection electric field pattern influences the thermospheric wind pattern through ion-neutral collisions.
- Interplay between the convection electric field and the thermospheric wind determines the ionospheric density variability, such as that within SED.
- Quantifying the roles of different formation mechanisms at different locations during geomagnetic active periods is a very active research topic.

Effects Part 3: Structuring the Polar Cap Ionosphere

Polar Cap Patches

White light ASI

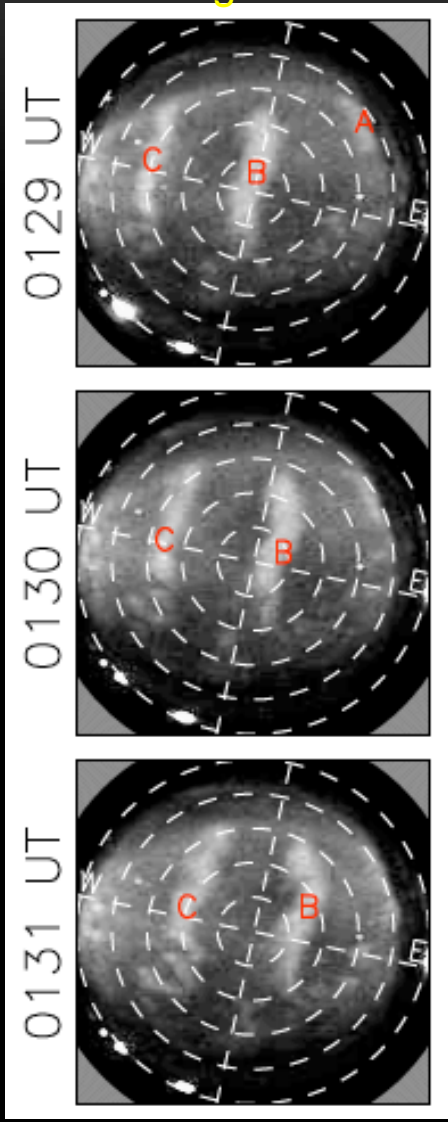

Hosokawa et al., 2010

RISR-N

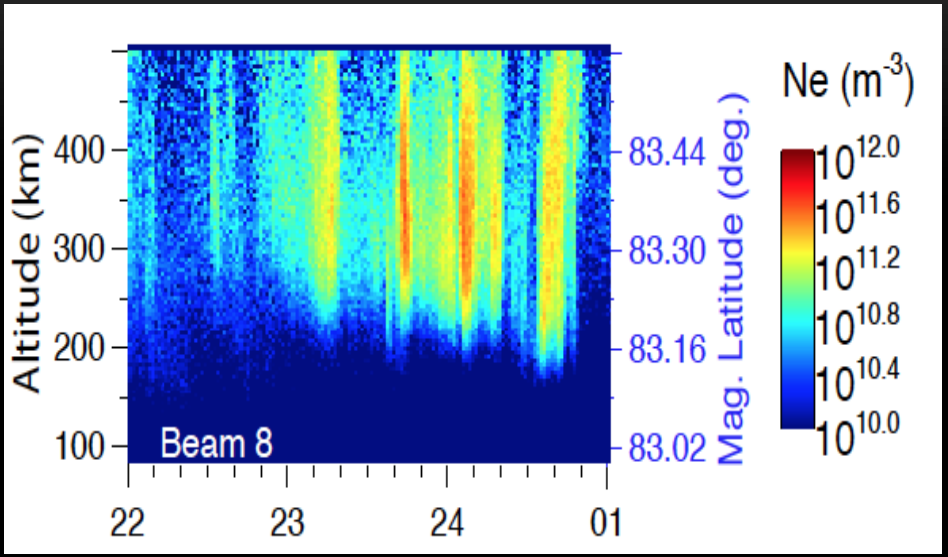

Zou et al., 2014

- Plasma patches are regions of enhanced plasma density (at least a factor of 2 greater than background densities) at polar latitudes.

Formation Mechanisms of Polar Cap Patches

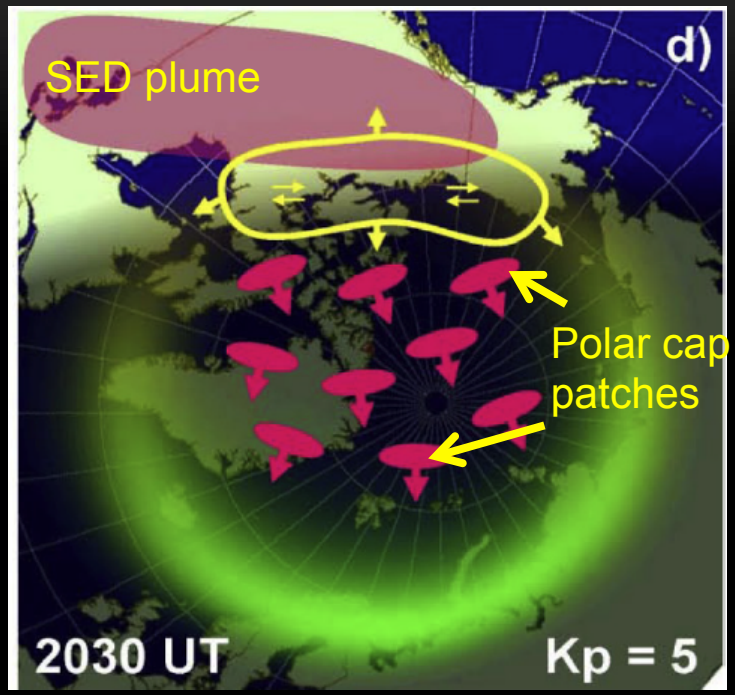

Moen et al., 2013

- Various formation mechanisms of patches have been proposed [*Carlson*, 2012 and references therein]:
  - Time dependent reconnection and pulsating soft electron precipitation
  - Sudden expansion and contraction of the convection pattern
  - IMF By direction changes
  - Enhanced recombination within high speed convection flows creating low density regions

There is evidence for each mechanism. But which one is responsible for the majority of the patches?

Seasonal and UT Dependence of Patches

model

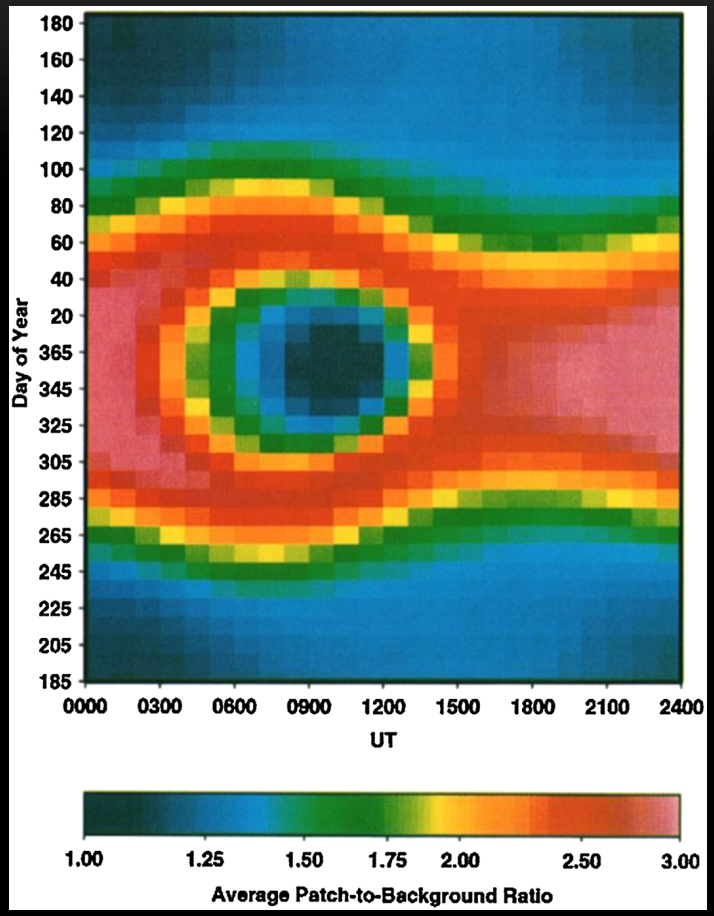

Sojka et al. 1994

GPS TEC

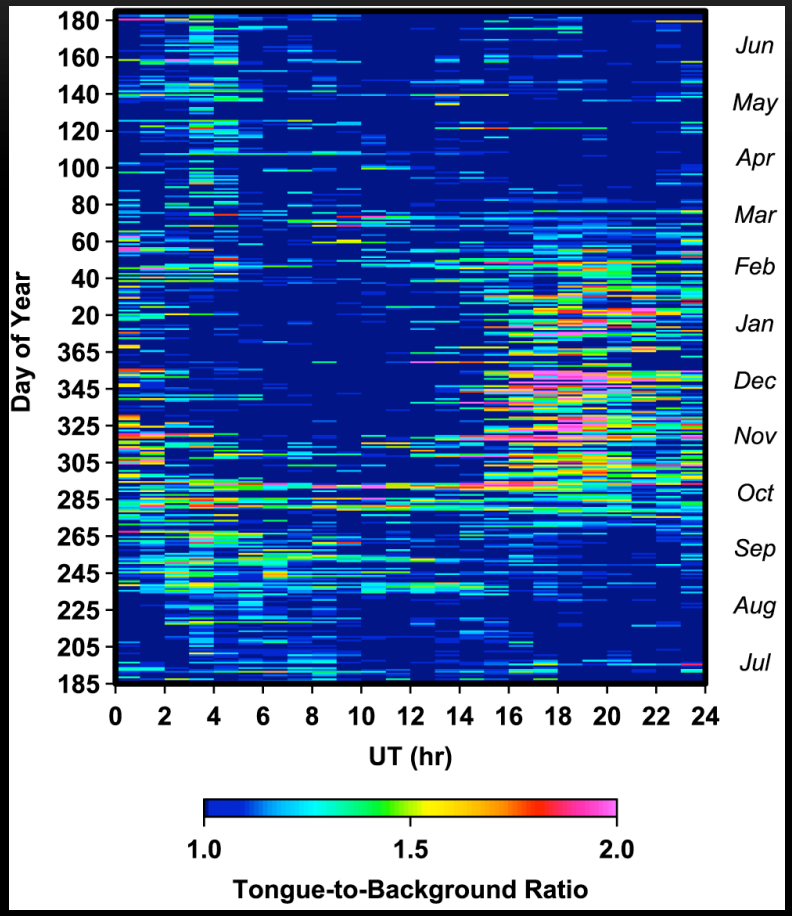

David et al. 2016

- Patches preferentially occur during winter and during 12-24 UT
  [*Coley and Heelis,* 1998; *David et al.* 2016].

Patches Drift at Convection Speed

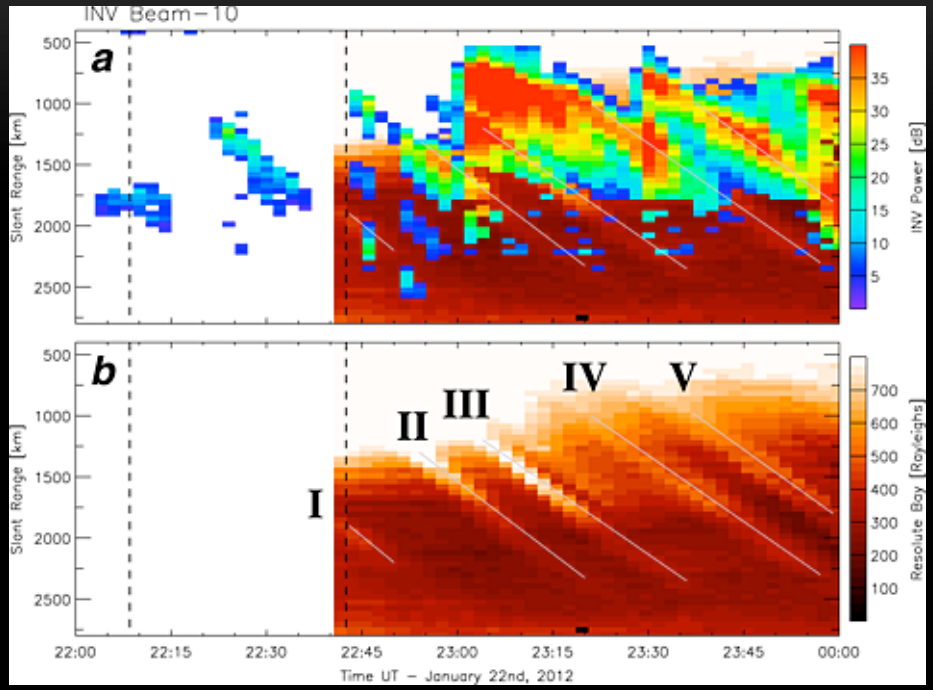

Table 1. Velocity Magnitudes of Polar Cap Patches Shown in Figure 3 as Determined From Great Circle Distance of Optical Traces and Averaged HF Radar Measurements

	Velocity (m/s)	
Patch	RSB (airglow)	INV (HF radar)
I	671	667
II	694	685
III	638	639
IV	612	665
V	647	679

Thomas et al., 2015

- A one-to-one spatial correspondence between the SuperDARN power and ASI airglow for the optical patches
- The motion of the optical patches has been shown to be consistent with the background plasma convection.
- Patches can be used as tracers of polar cap convection.

Patches as Tracers of Convection Flows

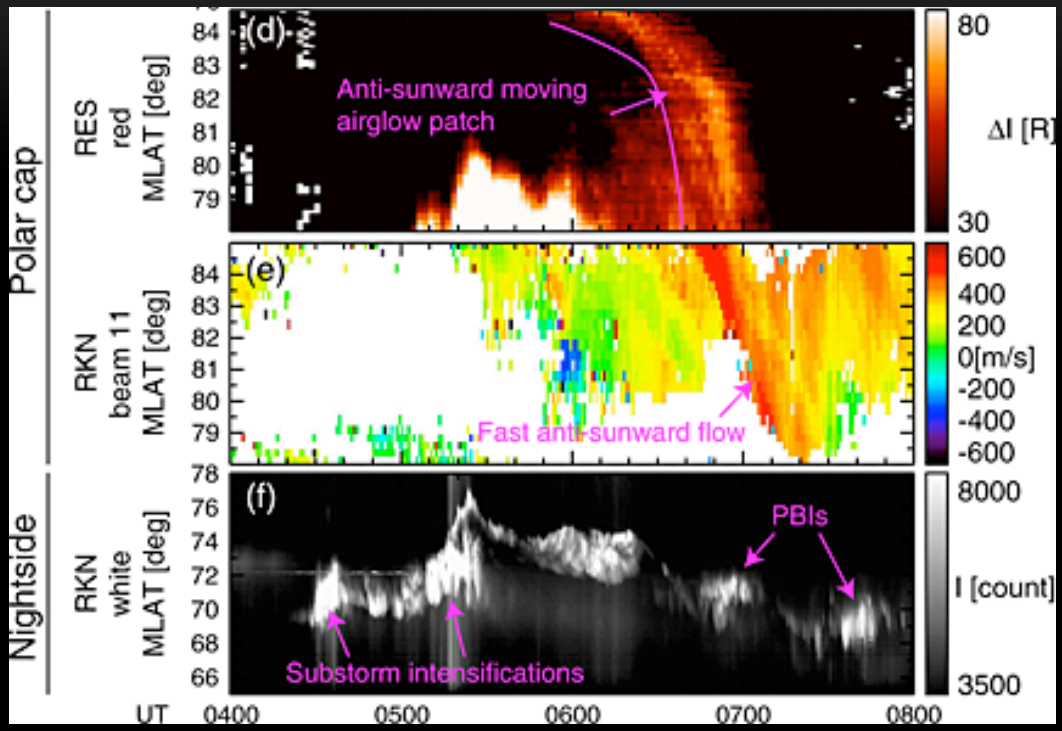

Nishimura et al., 2014

- Optical emission from patches has been used as tracers of convection flows to study the day-night coupling [*Nishimura et al.*, 2014], and evolution of meso-scale fast flow channels [*Zou Y. et al.*, 2015].

Auroral and Boundary Blobs

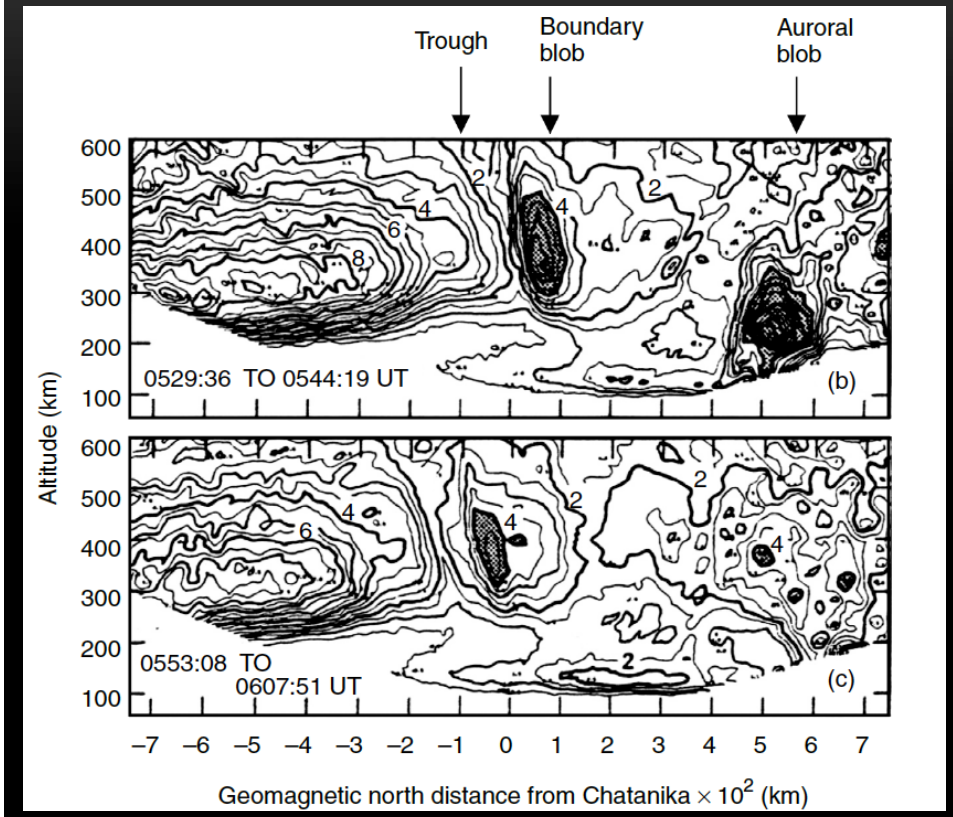

Crowley et al., 1996

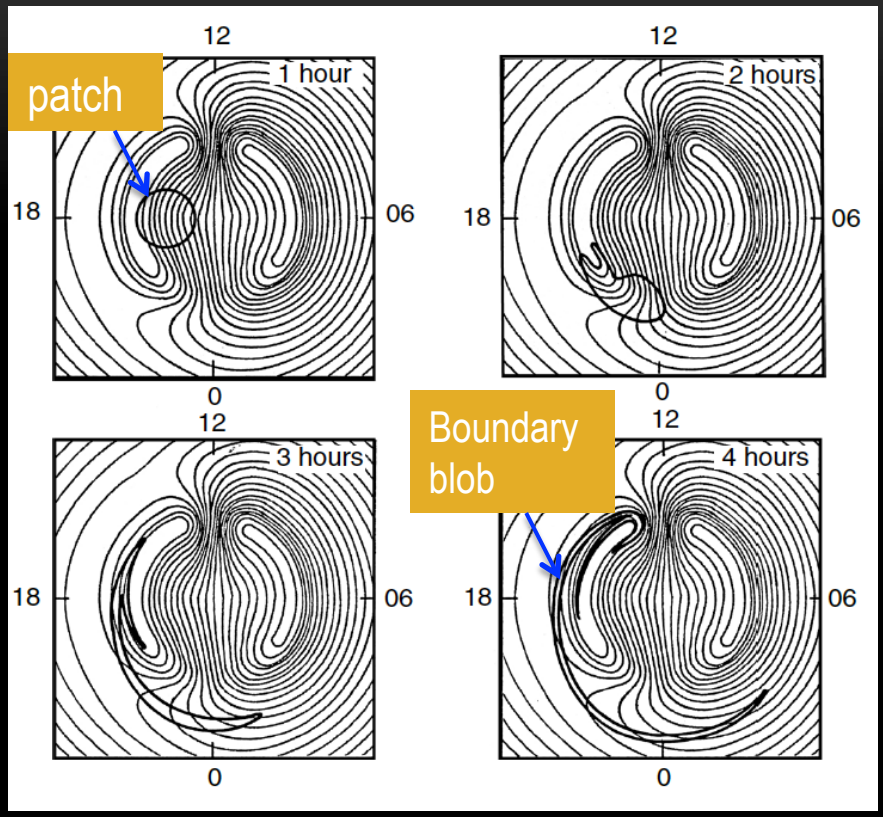

Crowley et al., 1996

- Boundary and auroral blobs are regions of enhanced plasma density that are located either inside of or on the equatorward edge of the auroral oval.
- Boundary blobs are not created locally. They are polar cap patches that have convected through the nightside auroral oval and subsequently moved around towards dusk.

Polar Cap Patch Circulation

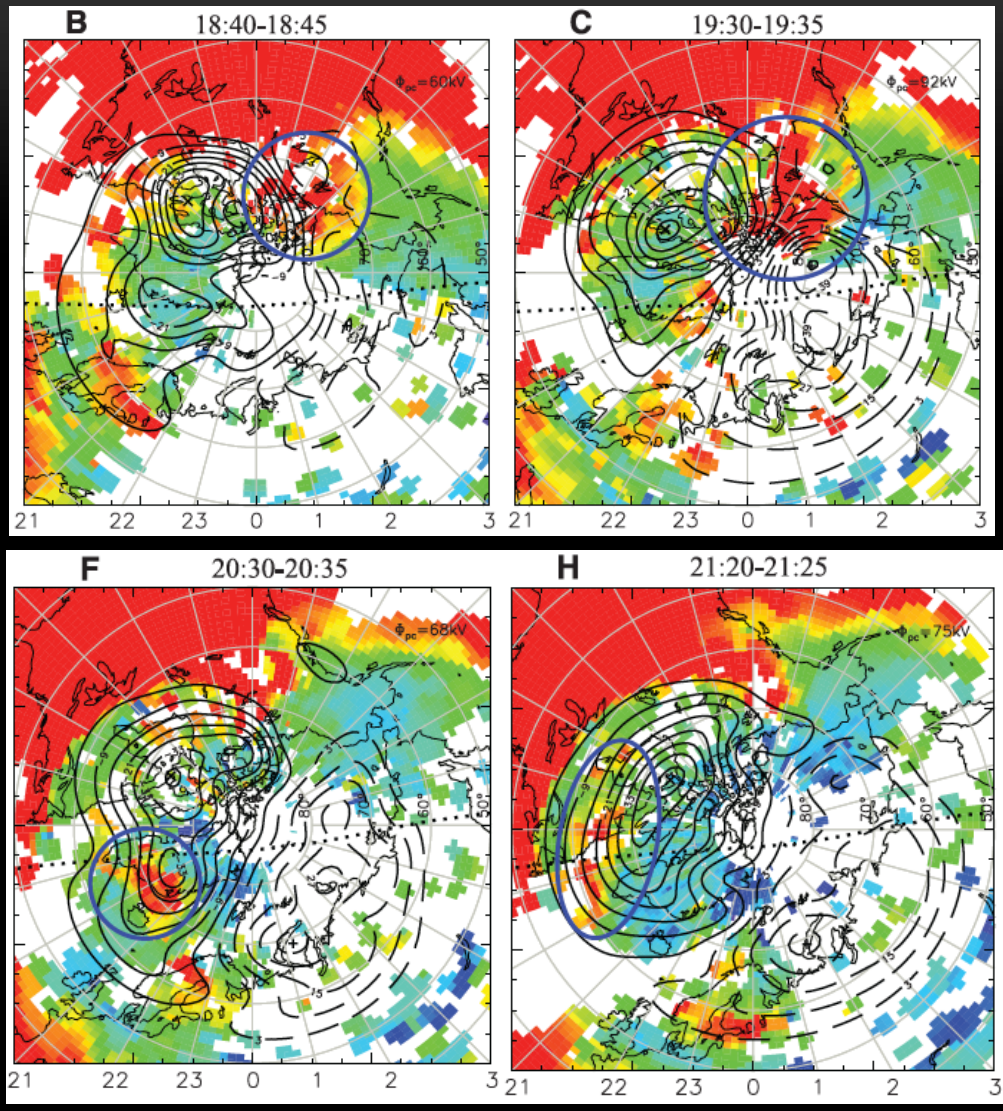

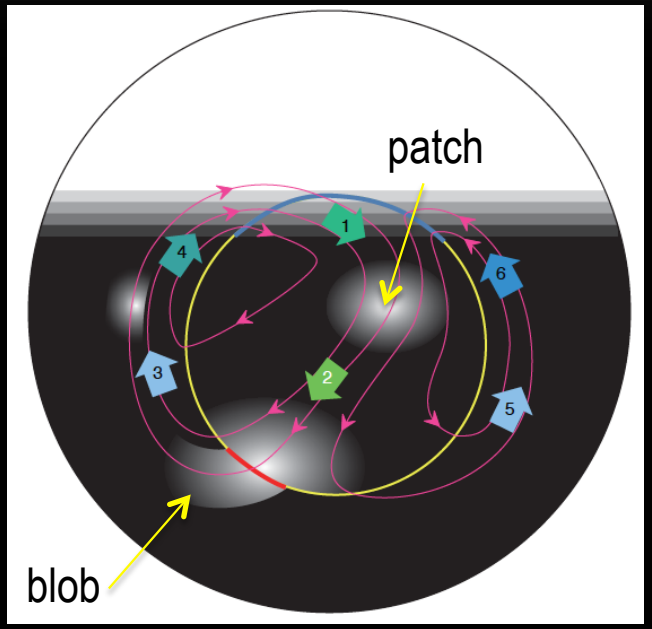

Zhang et al., 2013

Summary Part 2

- Convection electric field in the dayside cusp region is crucial for the formation of polar cap patches.
- After formation, patches drift anti-sunward at convection speed and can be used as tracers of convection flows.
- Patches are important plasma sources for the polar cap and nightside ionosphere.
- Open Question:
  - What is the major formation mechanism for polar cap patches?
  - How do polar cap patches exit the nightside polar cap?

Effects Part 4: Ion-Neutral Coupling within SAPS/SAID

SubAuroral Polarization Stream (SAPS) and SubAuroral Ion Drift (SAID)

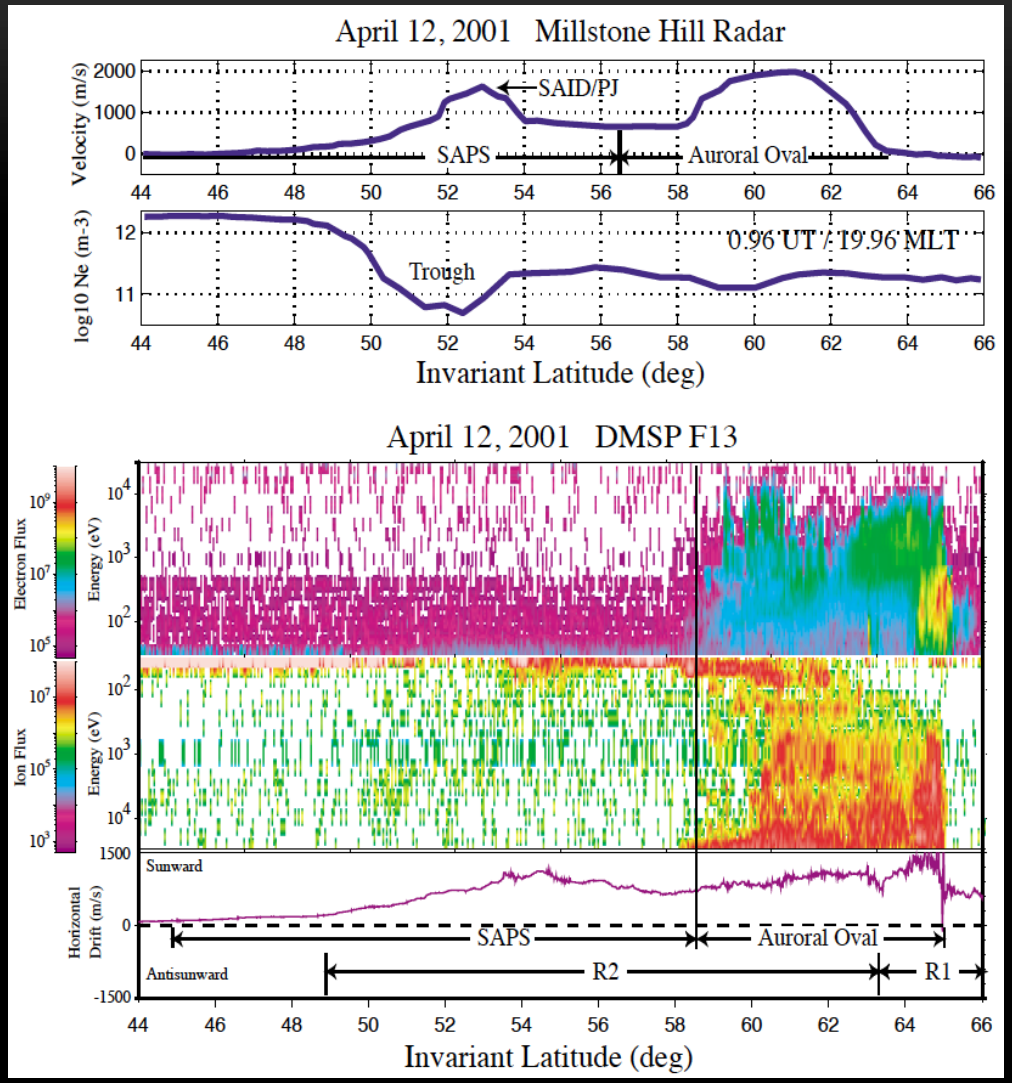

- SAPS: Enhanced convection flows equatorward of duskside electron precipitation.
- SAID is a narrower region within SAPS where the flow speed is higher.

Foster and Burke, 2002

Formation Mechanisms of SAPS and SAID

- *Southwood and Wolf* [1978] suggested that large SAPS electric fields arise as a result of the closure of downward Region-2 FACs in the low conductance ionosphere. In this scenario, ionosphere plays a passive role.
- *Banks and Yasuhara* [1978] suggested that poleward transport due to large poleward electric field in the subauroral E region can decrease the density and conductance.
- *Schunk et al.* [1976] suggested that frictional heating increases ion temperature and then increase the recombination rate and reduce the density and conductance.
- The latter two scenarios emphasize the role of positive feedback between the ionosphere and magnetosphere.

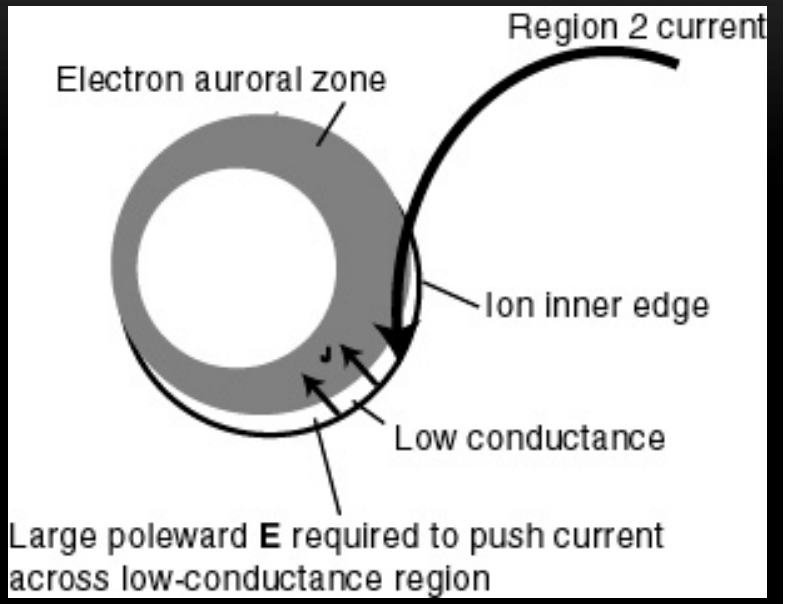

Wolf, 2002 GEM Tutorial

Composition Change due to Large Electric Fields

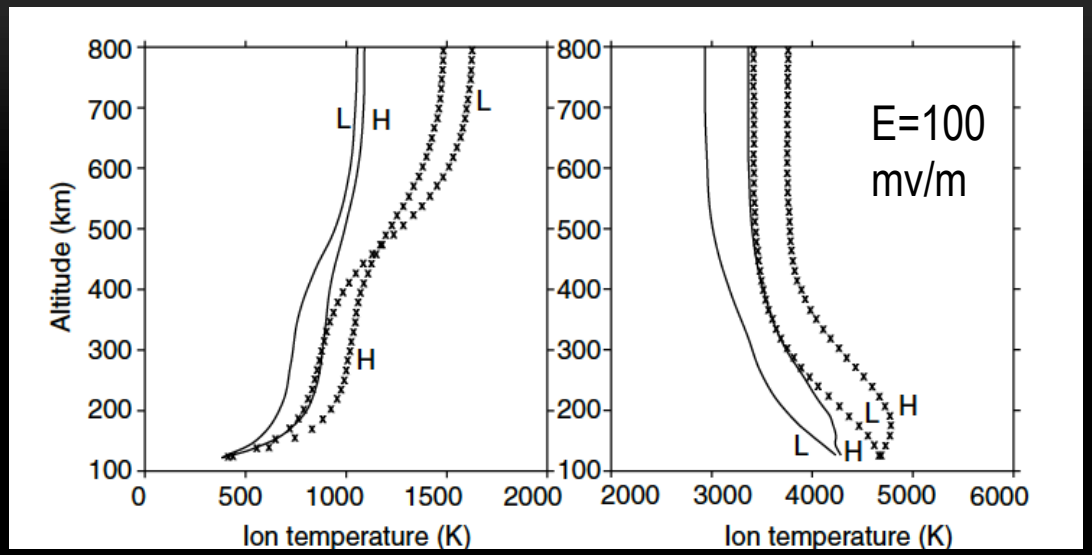

- Large electric field leads to fast conversion from O^+ to NO^+.
- Dissociative recombination of NO^+ is much faster than radiative recombination of O+.
- The electron density decreases rapidly.

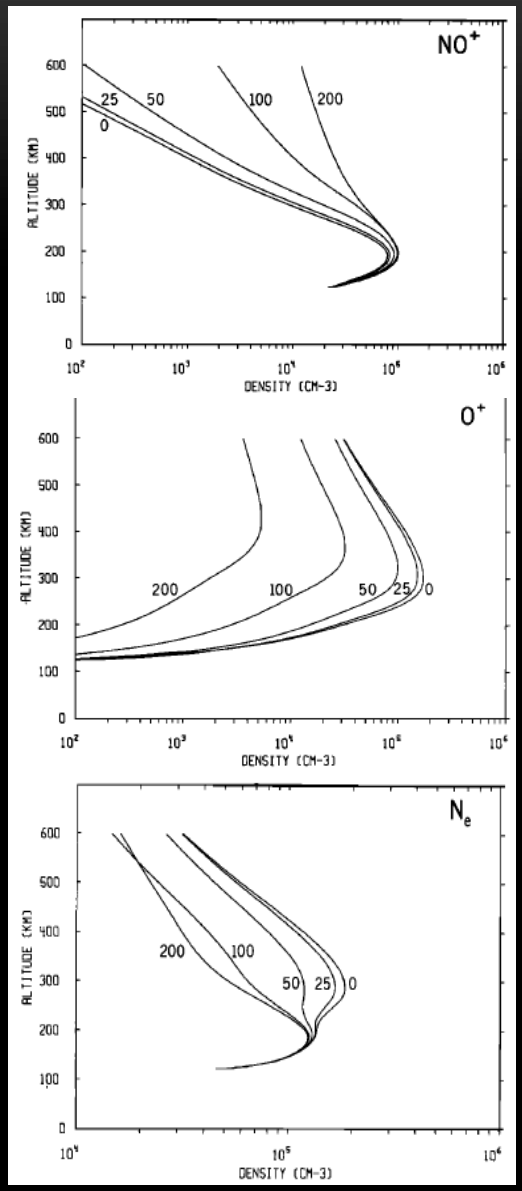

Schunk et al., 1975

Creation of Plasma Density Troughs

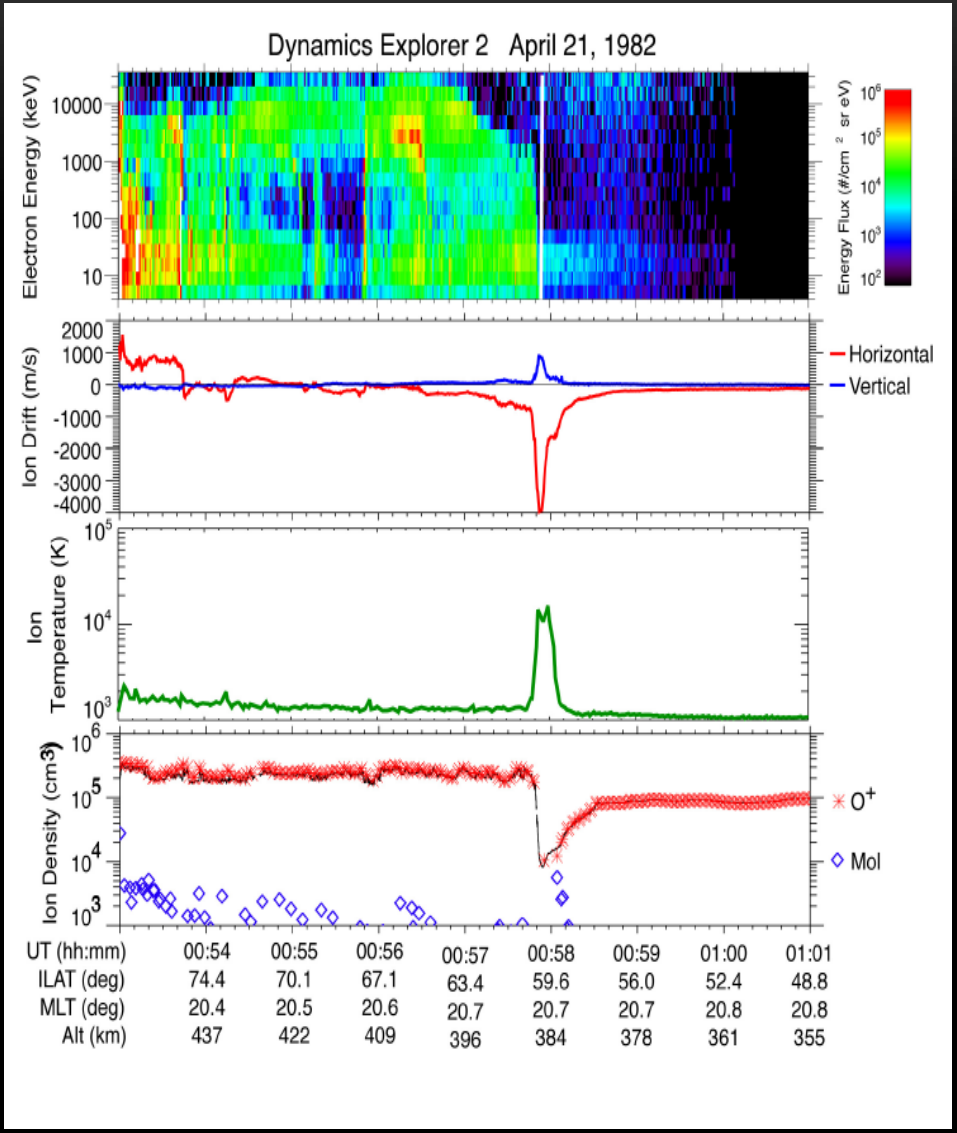

Courtesy: Rod Heelis

- Large horizontal ion drift near the equatorward boundary of precipitating electrons
- Ion temperature >10000K
- O^+ converted to NO^+
- Total ion density decreases

SAPS Evolution during Geomagnetic Substorms

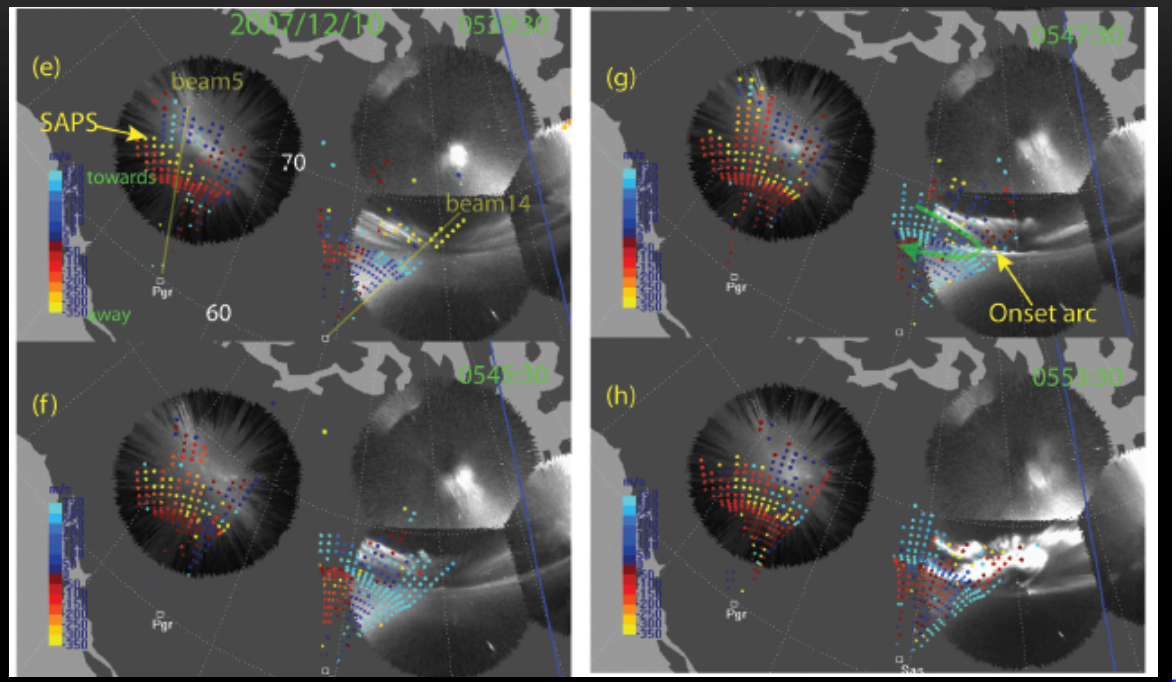

Zou et al., 2012

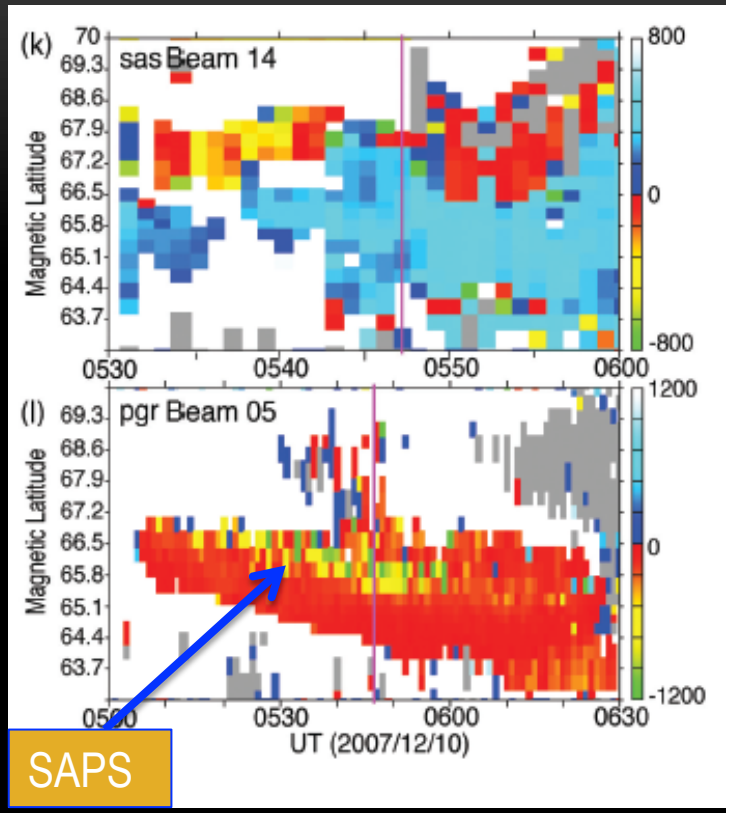

- SAPS forms during the growth phase of substorm as part of the Harang reversal [*Zou et al.* 2009, 2012; *Bristow and Jensen*, 2007].

SAPS Response to Substorm Westward Traveling Surge (WTS)

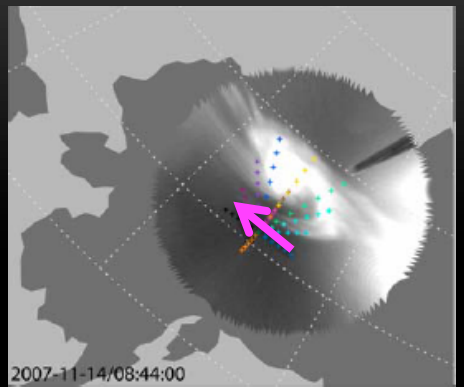

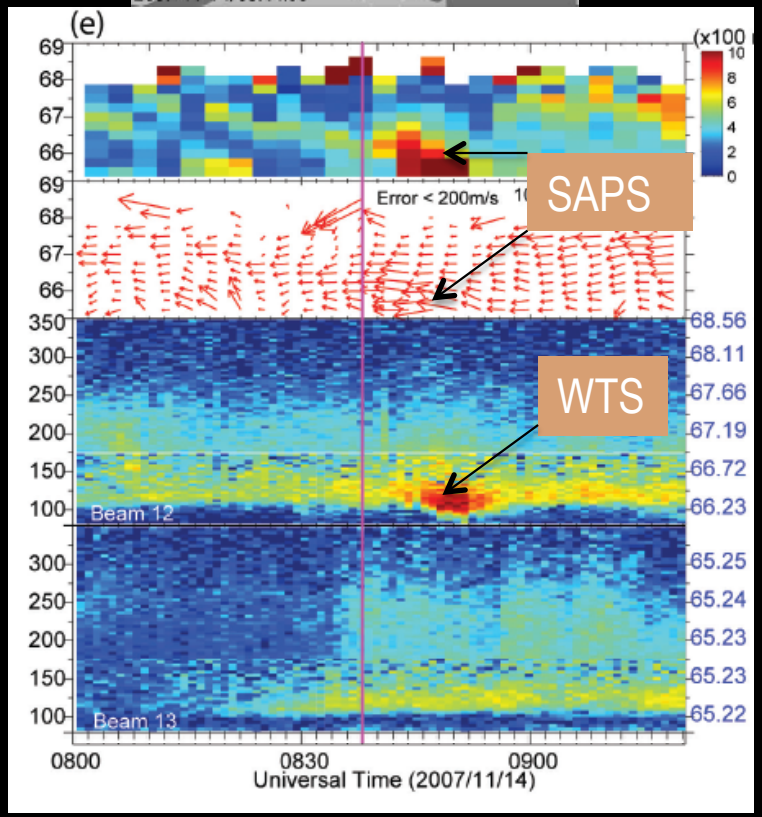

Zou et al., 2009

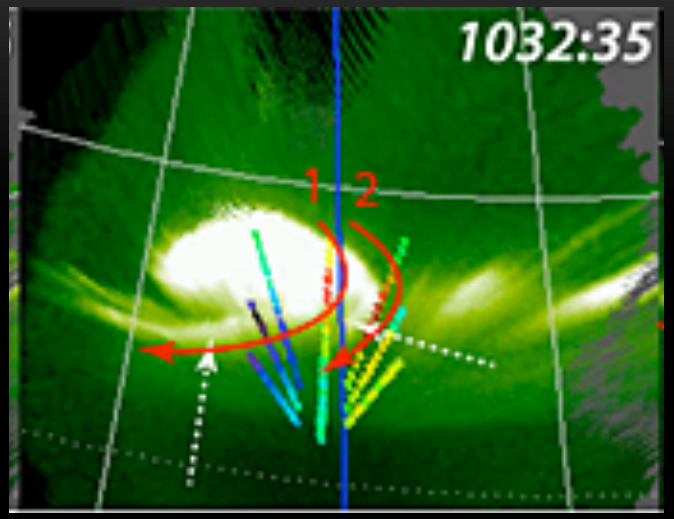

Lyons et al,. 2015

- SAPS increases when WTS moves into the same MLT but at higher latitude [*Zou et al.*, 2009].
- Highly varying SAPS responses to the fine structures within WTS observed [*Lyons et al.*, 2015].

Fine Structure of Ring Current

BATSRUS +CRCM simulation

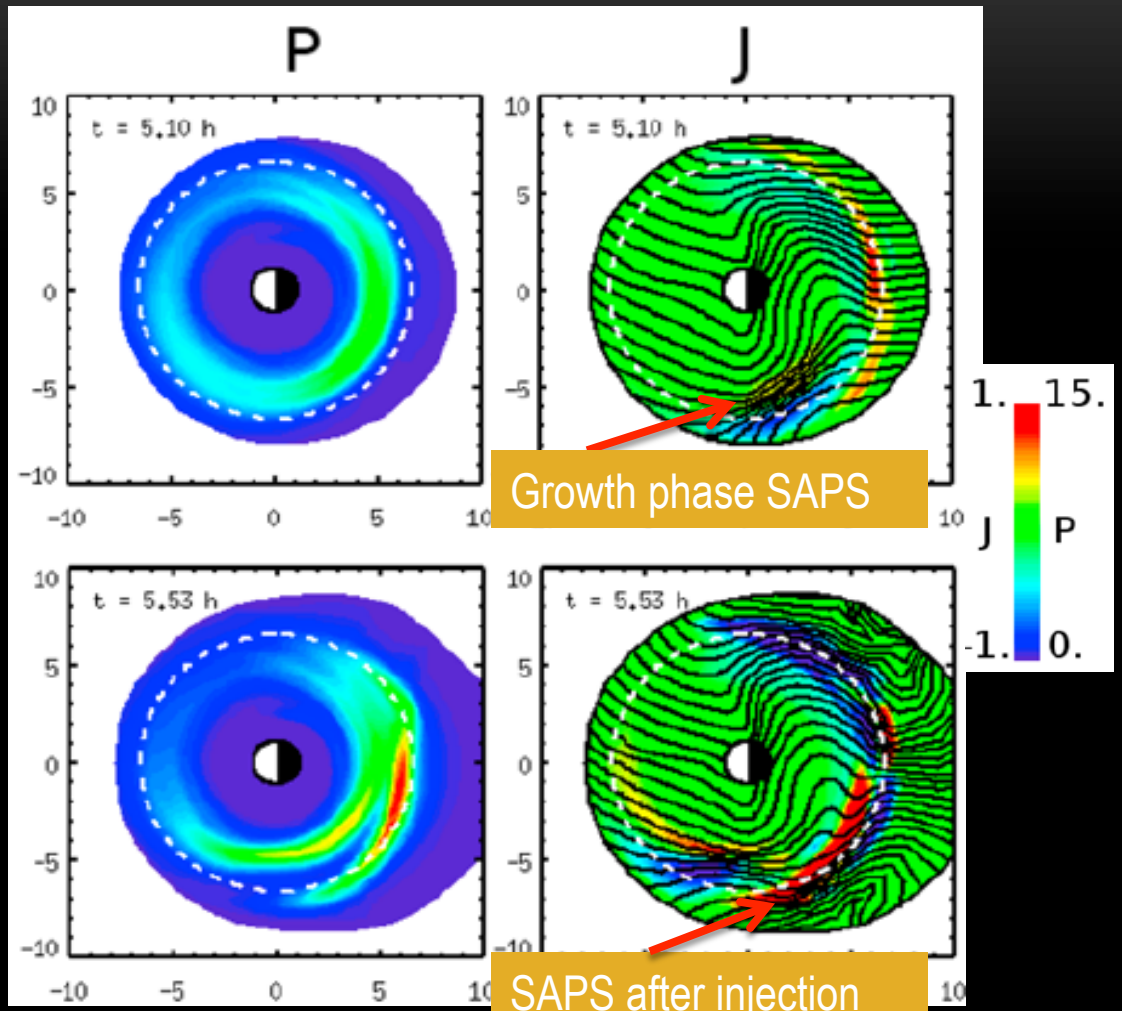

Buzulukova et al., 2010

- Complex structure of the ring current and Region-2 FACs seen in RCM [*Yang et al.*, 2008] and CRCM [*Buzulukova et al.*, 2008, 2010] simulations.

Effects of Proton Precipitation in SAPS

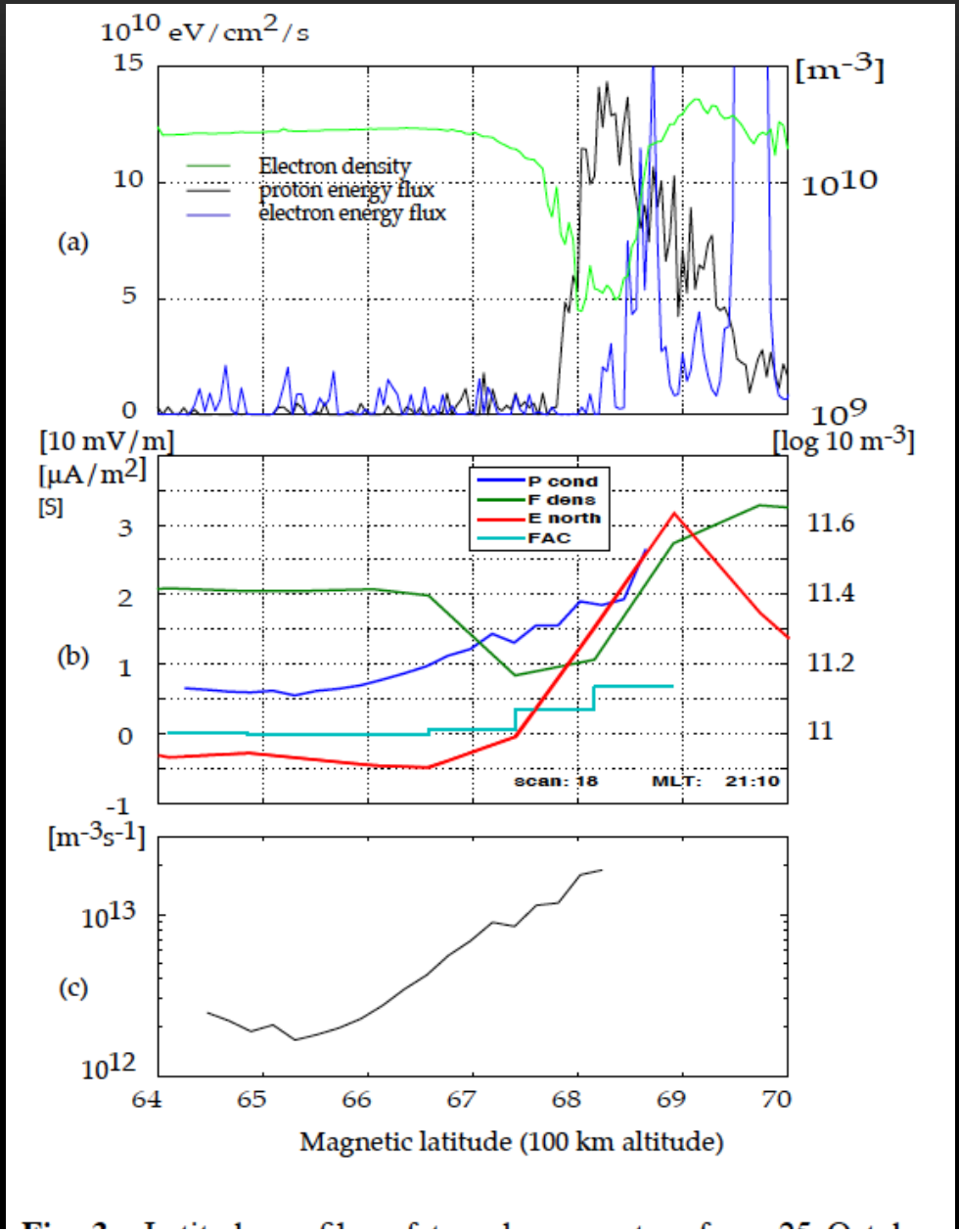

- Proton precipitation within SAPS can increase conductance and suppress the SAPS electric field.
- Topside ionosphere shows a density trough but not a local dip in the E region.
- Be cautious about the altitude of the trough associated with SAPS.
- Proton precipitation should be included in the SAPS modeling.

Nilsson et al., 2005

Summary Part 4

- SAPS/SAID are unique convection flow structures reflecting the feedbacks between the magnetosphere-ionosphere-thermosphere coupling.
- Observationally, latitudinal profile of conductivity within SAPS is needed to identify the formation mechanism.
- Successfully modeling the formation and evolution of SAPS/SAID requires to include 2-way coupling between magnetosphere-ionosphere-thermosphere.
  - Self-consistent conductance, including both electrons and protons
  - Particle injection in the inner magnetosphere and the formation of structured partial ring current
  - Plasma temperature dependent chemical reactions

Summary

Drivers:

- High-latitude ionospheric convection dynamically responds to solar wind and IMF drivers.
  - Reconnection
  - Viscous Interaction
- Hot plasma in the magnetosphere modifies the convection pattern through the closure of field-aligned currents in the ionosphere.
  - Region-2 FACs
  - Harang reversal and SAPS

Effects:

- Neutral dynamics effects
- Uplifting/downshifting effects
- Structuring the polar cap ionosphere
- Ion-neutral coupling within SAPS/SAID

References part 1:

1. Axford, W. I. (1964), Viscous interaction between the solar wind and the earth's magnetosphere, *Planetary and Space Science*, *12*(1), 45–53, doi:10.1016/0032-0633(64)90067-4.
2. Buzulukova, N., and V. Vovchenko (2008), Modeling of proton nose structures in the inner magnetosphere with a self-consistent electric field model, *Journal of Atmospheric and Solar-Terrestrial Physics*, *70*(2-4), 503–510, doi:10.1016/j.jastp.2007.08.028.
3. Buzulukova, N., M.-C. Fok, A. Pulkkinen, M. Kuznetsova, T. E. Moore, A. Glocer, P. C. Brandt, G. Tóth, and L. Rastätter (2010), Dynamics of ring current and electric fields in the inner magnetosphere during disturbed periods: CRCM-BATS-R-US coupled model, *Journal of Geophysical Research: Space Physics*, *115*(A5), n/a–n/a, doi:10.1029/2009JA014621.
4. *Bristow, W. A., and P. Jensen (2007), A superposed epoch study of SuperDARN convection observations during substorms, J. Geophys. Res., 112, A06232, doi:10.1029/2006JA012049.*
5. Carlson, H. C. (2012), Sharpening our thinking about polar cap ionospheric patch morphology, research, and mitigation techniques, *Radio Science*, *47*(4), doi:10.1029/2011RS004946.
6. Coley, W. R., and R. A. Heelis (1998), Structure and occurrence of polar ionization patches, *Journal of Geophysical Research: Space Physics*, *103*(A2), 2201–2208, doi:10.1029/97JA03345.
7. Crowley, G., Critical review of ionospheric patches and blobs, in *Review of Radio Science 1993–1996*, chapter 27, Ed. W.R., Stone, Oxford Science Publication, UK, 619–648, 1996.
8. David, M., J. J. Sojka, R. W. Schunk, and A. J. Coster (2016), Polar cap patches and the tongue of ionization: A survey of GPS TEC maps from 2009 to 2015, *Geophysical Research Letters*, *43*(6), 2422–2428, doi:10.1002/2016GL068136.
9. Dungey, J. W. (1961), Interplanetary Magnetic Field and the Auroral Zones, *Physical Review Letters*, *6*(2), 47–48, doi:10.1103/PhysRevLett.6.47.
10. Foster, J. C., and W. J. Burke (2002), SAPS: A new categorization for sub-auroral electric fields, *Eos, Transactions American Geophysical Union*, *83*(36), 393–394.
11. Gkioulidou, M., C.-P. Wang, L. R. Lyons, and R. A. Wolf (2009), Formation of the Harang reversal and its dependence on plasma sheet conditions: Rice convection model simulations, *Journal of Geophysical Research: Space Physics*, *114*(A7), n/a–n/a, doi:10.1029/2008JA013955.
12. Gkioulidou, M., C.-P. Wang, and L. R. Lyons (2011), Effect of self-consistent magnetic field on plasma sheet penetration to the inner magnetosphere: Rice convection model simulations combined with modified Dungey force-balanced magnetic field solver, *Journal of Geophysical Research: Space Physics*, *116*(A12), n/a–n/a, doi:10.1029/2011JA016810.
13. Heelis, R. A. (2004), Electrodynamics in the low and middle latitude ionosphere: a tutorial, *Journal of Atmospheric and Solar-Terrestrial Physics*, *66*(10), 825–838, doi:10.1016/j.jastp.2004.01.034.
14. Heelis, R. A., J. J. Sojka, M. David, and R. W. Schunk (2009), Storm time density enhancements in the middle-latitude dayside ionosphere, *Journal of Geophysical Research: Space Physics*, *114*(A3), n/a–n/a, doi:10.1029/2008JA013690.

References part 2:

15. Hosokawa, K., T. Motoba, A. S. Yukimatu, S. E. Milan, M. Lester, A. Kadokura, N. Sato, and G. Bjornsson (2010), Plasma irregularities adjacent to auroral patches in the postmidnight sector, *Journal of Geophysical Research: Space Physics*, *115*(A9), n/a–n/a, doi:10.1029/2010JA015319.
16. Huba, J. D., and S. Sazykin (2014), Storm time ionosphere and plasmasphere structuring: SAMI3-RCM simulation of the 31 March 2001 geomagnetic storm, *Geophysical Research Letters*, *41*(23), 8208–8214, doi:10.1002/2014GL062110.
17. Kivelson, M. G. and C. J. Russel (2005), *Introduction to space physics*, 1. publ., transferred to digital print., Cambridge Univ. Press.
18. Lu, G., L. Goncharenko, M. J. Nicolls, A. Maute, A. Coster, and L. J. Paxton (2012), Ionospheric and thermospheric variations associated with prompt penetration electric fields, *Journal of Geophysical Research: Space Physics*, *117*(A8), n/a–n/a, doi: 10.1029/2012JA017769.
19. Lu, G., Auroral Boundaries: Finding them in data and models, 2005, GEM.
20. Lyons, L. R., and D. J. Williams (1984), *Quantitative Aspects of Magnetospheric Physics*, Springer Netherlands, Dordrecht.
21. Lyons, L. R. et al. (2015), Azimuthal flow bursts in the inner plasma sheet and possible connection with SAPS and plasma sheet earthward flow bursts, *Journal of Geophysical Research: Space Physics*, *120*(6), 5009–5021, doi:10.1002/2015JA021023.
22. Moen, J., K. Oksavik, L. Alfonsi, Y. Daabakk, V. Romano, and L. Spogli (2013), Space weather challenges of the polar cap ionosphere, *Journal of Space Weather and Space Climate*, *3*, A02, doi:10.1051/swsc/2013025.
23. Nilsson, H., T. I. Sergienko, Y. Ebihara, and M. Yamauchi (2005), Quiet-time mid-latitude trough: influence of convection, field-aligned currents and proton precipitation, in *Annales Geophysicae*, vol. 23, pp. 3277–3288.
24. Nishimura, Y. et al. (2014), Day-night coupling by a localized flow channel visualized by polar cap patch propagation, *Geophysical Research Letters*, *41*(11), 3701–3709, doi:10.1002/2014GL060301.
25. Reiff, P. H. (1982), Sunward convection in both polar caps, *Journal of Geophysical Research*, *87*(A8), 5976, doi:10.1029/JA087iA08p05976.
26. Richmond, A. D., and R. G. Roble (1997), Electrodynamic coupling effects in the thermosphere/ionosphere system, *Advances in Space Research*, *20*(6), 1115–1124, doi:10.1016/S0273-1177(97)00754-0.
27. Schunk, R. W., W. J. Raitt, and P. M. Banks (1975), Effect of electric fields on the daytime high-latitude *E* and *F* regions, *Journal of Geophysical Research*, *80*(22), 3121–3130, doi:10.1029/JA080i022p03121.
28. Schunk, R. W. and A. Nagy (2009), Ionospheres, Cambridge Univ. Press, Cambridge
29. Sojka, J. J., M. D. Bowline, and R. W. Schunk (1994), Patches in the polar ionosphere: UT and seasonal dependence, *Journal of Geophysical Research*, *99*(A8), 14959, doi:10.1029/93JA03327.
30. Thomas, E. G. et al. (2015), Multi-instrument, high-resolution imaging of polar cap patch transportation, *Radio Science*, *50*(9), 904–915, doi:10.1002/2015RS005672.

References part 3:

31. Weimer, D. R. (1995), Models of high-latitude electric potentials derived with a least error fit of spherical harmonic coefficients, *Journal of Geophysical Research*, *100*(A10), 19595, doi:10.1029/95JA01755.
32. Wolf, R. A., R. W. Spiro, S. Sazykin, and F. R. Toffoletto (2007), How the Earth's inner magnetosphere works: An evolving picture, *Journal of Atmospheric and Solar-Terrestrial Physics*, *69*(3), 288–302, doi:10.1016/j.jastp.2006.07.026.
33. Wolf, R. A., Inner Magnetospheric Electric Field, 2002, GEM.
34. Yang, J., F. R. Toffoletto, R. A. Wolf, S. Sazykin, R. W. Spiro, P. C. Brandt, M. G. Henderson, and H. U. Frey (2008), Rice Convection Model simulation of the 18 April 2002 sawtooth event and evidence for interchange instability, *Journal of Geophysical Research: Space Physics*, *113*(A11), n/a–n/a, doi:10.1029/2008JA013635.
35. Zhang, Q.-H. et al. (2013), Direct Observations of the Evolution of Polar Cap Ionization Patches, *Science*, *339*(6127), 1597–1600, doi:10.1126/science.1231487.
36. Zou, S., L. R. Lyons, M. J. Nicolls, C. J. Heinselman, and S. B. Mende (2009), Nightside ionospheric electrodynamics associated with substorms: PFISR and THEMIS ASI observations, *Journal of Geophysical Research: Space Physics*, *114*(A12), n/a–n/a, doi: 10.1029/2009JA014259.
37. Zou, S., L. R. Lyons, and Y. Nishimura (2012), Mutual Evolution of Aurora and Ionospheric Electrodynamic Features Near the Harang Reversal During Substorms, in *Geophysical Monograph Series*, vol. 197, edited by A. Keiling, E. Donovan, F. Bagenal, and T. Karlsson, pp. 159–169, American Geophysical Union, Washington, D. C.
38. Zou, S., A. J. Ridley, M. B. Moldwin, M. J. Nicolls, A. J. Coster, E. G. Thomas, and J. M. Ruohoniemi (2013), Multi-instrument observations of SED during 24-25 October 2011 storm: Implications for SED formation processes, *Journal of Geophysical Research: Space Physics*, *118*(12), 7798–7809, doi:10.1002/2013JA018860.
39. Zou, S., M. B. Moldwin, A. J. Ridley, M. J. Nicolls, A. J. Coster, E. G. Thomas, and J. M. Ruohoniemi (2014), On the generation/decay of the storm-enhanced density plumes: Role of the convection flow and field-aligned ion flow: Generation and Decay of SED Plumes, *Journal of Geophysical Research: Space Physics*, *119*(10), 8543–8559, doi:10.1002/2014JA020408.
40. Zou, S., S. Y. Tafti, M. B. Moldwin, A. J. Ridley, M. J. Nicolls (2014), RISR-N Observation of the Characteristics of Polar Cap Patches and Implication for Patch Formation Mechanism, *AGU, Fall meeting 2014*.
41. Zou, S. and A. Ridley (2015), Modeling of the evolution of Storm-Enhanced Density (SED) plume during the Oct. 24-25, 2011 geomagnetic storm, AGU Monograph of Yosemite Chapman Conference on "*Magnetosphere and Ionosphere Coupling in the Solar System*", accepted, ISBN: 978-1-119-06677-4.
42. Zou, Y., Y. Nishimura, L. R. Lyons, K. Shiokawa, E. F. Donovan, J. M. Ruohoniemi, K. A. McWilliams, and N. Nishitani (2015), Localized polar cap flow enhancement tracing using airglow patches: Statistical properties, IMF dependence, and contribution to polar cap convection. *J. Geophys. Res. Space Physics, 120*, 4064–4078. doi: 10.1002/2014JA020946.